

A new feature in the internal heavy isotope distribution in ozone

S. K. Bhattacharya, Joel Savarino, G. Michalski, and Mao-Chang Liang

Citation: *The Journal of Chemical Physics* **141**, 134301 (2014); doi: 10.1063/1.4895614

View online: <http://dx.doi.org/10.1063/1.4895614>

View Table of Contents: <http://scitation.aip.org/content/aip/journal/jcp/141/13?ver=pdfcov>

Published by the [AIP Publishing](#)

Articles you may be interested in

[An approximate theory of the ozone isotopic effects: Rate constant ratios and pressure dependence](#)

J. Chem. Phys. **127**, 244316 (2007); 10.1063/1.2806189

[Macroscopic evidences for non-Rice-Ramsperger-Kassel effects in the reaction between \$\text{H}_3\text{O}^+\$ and \$\text{D}_2\text{O}\$: The occurrence of nonstatistical isotopic branching ratio](#)

J. Chem. Phys. **126**, 204305 (2007); 10.1063/1.2742381

[The effect of zero-point energy differences on the isotope dependence of the formation of ozone: A classical trajectory study](#)

J. Chem. Phys. **122**, 094317 (2005); 10.1063/1.1860011

[Some symmetry-induced isotope effects in the kinetics of recombination reactions](#)

J. Chem. Phys. **121**, 800 (2004); 10.1063/1.1758697

[An intramolecular theory of the mass-independent isotope effect for ozone. I](#)

J. Chem. Phys. **111**, 4087 (1999); 10.1063/1.480267



A new feature in the internal heavy isotope distribution in ozone

S. K. Bhattacharya,^{1,a)} Joel Savarino,² G. Michalski,³ and Mao-Chang Liang¹

¹Research Center for Environmental Changes, Academia Sinica, Taipei, Taiwan

²Laboratoire de Glaciologie et Géophysique de l'Environnement, CNRS, Université Joseph Fourier-Grenoble, 54 rue Molière BP96, St Martin d'Heres, 38402, France

³Department of Earth and Atmospheric Sciences, Purdue University, Indiana 47906, USA

(Received 8 March 2014; accepted 2 September 2014; published online 1 October 2014)

Ozone produced by discharge or photolysis of oxygen has unusually heavy isotopic composition ($^{18}\text{O}/^{16}\text{O}$ and $^{17}\text{O}/^{16}\text{O}$ ratio) which does not follow normal mass fractionation rule: $\delta^{17}\text{O} \sim 0.52 * \delta^{18}\text{O}$, expressed as an anomaly $\Delta^{17}\text{O} = \delta^{17}\text{O} - 0.52 * \delta^{18}\text{O}$. Ozone molecule being an open isosceles triangle can have the heavy isotope located either in its apex or symmetric (s) position or the base or asymmetric (as) position. Correspondingly, one can define positional isotopic enrichment, written as $\delta^{18}\text{O}$ (s) or $\delta^{18}\text{O}$ (as) (and similarly for $\delta^{17}\text{O}$) as well as position dependent isotope anomaly $\Delta^{17}\text{O}$ (s) and $\Delta^{17}\text{O}$ (as). Marcus and co-workers have proposed a semi-empirical model based in principle on the RRKM model of uni-molecular dissociation but with slight modification (departure from statistical randomness assumption for symmetrical molecules) which explains many features of ozone isotopic enrichment. This model predicts that the bulk isotope anomaly is contained wholly in the asymmetric position and the $\Delta^{17}\text{O}$ (s) is zero. Consequently, $\Delta^{17}\text{O}$ (as) = $1.5 * \Delta^{17}\text{O}$ (bulk) (named here simply as the “1.5 rule”) which has been experimentally confirmed over a range of isotopic enrichment. We now show that a critical re-analysis of the earlier experimental data demonstrates a small but significant departure from this 1.5 rule at the highest and lowest levels of enrichments. This departure provides the first experimental proof that the dynamics of ozone formation differs from a statistical model constrained only by restriction of symmetry. We speculate over some possible causes for the departure. © 2014 AIP Publishing LLC. [<http://dx.doi.org/10.1063/1.4895614>]

I. INTRODUCTION

Several experimental studies have demonstrated that ozone formed by gas phase recombination reaction of oxygen atom (O) and molecule (O_2) is unusually enriched in heavy isotopes ^{17}O and ^{18}O compared to the initial oxygen reservoir.³⁶ A similar effect has been found in natural ozone formed in troposphere or stratosphere.²⁵ In the following we use the standard delta notation to express heavy isotope ratios of a sample in per mil (‰):

$$\delta^x\text{O} = [({}^x\text{O}/^{16}\text{O})_{\text{spl}} / ({}^x\text{O}/^{16}\text{O})_{\text{ref}} - 1] * 1000, \quad (1)$$

where $x = 17$ or 18 ; the subscript “spl” refers to an oxygen sample and “ref” to an oxygen standard providing a reference ratio. If the reference oxygen gas constitutes the reservoir from which ozone is made the δ -values would also indicate enrichment/depletion. This was the case in the present experimental work. Naturally, the composition of the starting gas was also used as the reference in the chemical model discussed later. Experimentally, the $\delta^{17}\text{O}$ or $\delta^{18}\text{O}$ values of ozone formed in gas phase reactions could be as high as 150‰. It was noted by Morton *et al.*³² that δ -values increase with temperature and decrease with pressure in the reservoir. In addition, the ozone formed by discharge or oxygen photol-

ysis has a second unusual feature. The enrichments in ^{17}O and ^{18}O do not obey the usual mass dependence (MD) relation (Miller²⁹): $1000 * \ln(1 + \delta^{17}\text{O}/1000) = 0.52 * 1000 * \ln(1 + \delta^{18}\text{O}/1000)$. In the present paper, we shall use this relation in its simple linearized form: $\delta^{17}\text{O} = 0.52 * \delta^{18}\text{O}$ because the error introduced by the linearization is small compared to the dispersion in our experimental data and the smoothing error. Thieme and Heidenreich³⁶ found that instead of a MD relation, the $\delta^{17}\text{O}$ of ozone is nearly equal to its $\delta^{18}\text{O}$. This is indicative of an unusual mass independent fractionation and its magnitude is expressed by ^{17}O -excess or isotopic anomaly defined as: $\Delta^{17}\text{O} = \delta^{17}\text{O} - 0.52 * \delta^{18}\text{O}$ which expresses the deviation of $\delta^{17}\text{O}$ from its expected value based on the MD law. These two features, namely the heavy isotopic enrichment and isotopic anomaly (as defined above) correlate with each other and were explained by a semi-empirical model proposed by Hathorn and Marcus^{12,13} and Gao and Marcus⁹ denoted hereafter as HGM model.

There is a third subtle aspect in the isotopic enrichment concerning positional δ -values. Ozone being a triangular open molecule (with apex angle of about 116°) the heavy isotopic species can have ^{17}O or ^{18}O located in the apex position (forming a symmetric molecule) or in one of the two base positions (forming an asymmetric molecule). Here we neglect species with two or more heavy isotopes in a single molecule since their abundance is small when formed from natural oxygen. Therefore, in addition to the bulk enrichment, one can consider enrichment of the two individual isotopomers

^{a)} Author to whom correspondence should be addressed. Electronic mail: skbhatta1@gmail.com.

of ozone, one pair for each of the two heavy isotopes. For example, in case of ^{18}O -species, abundance of $^{16}\text{O}^{18}\text{O}^{16}\text{O}$ type (symmetric) molecule or $^{16}\text{O}^{16}\text{O}^{18}\text{O}$ type (asymmetric) molecule can be higher compared to that based on a random distribution of the ^{16}O and ^{18}O atoms (with ^{18}O in the apex or base position, respectively) derived from the parent oxygen reservoir. If the heavy isotope distribution were totally random one would expect $r_{50} = [^{16}\text{O}^{16}\text{O}^{18}\text{O}]/[^{16}\text{O}^{18}\text{O}^{16}\text{O}]$ ratio to be exactly two as dictated by the binomial distribution of ^{18}O in the triangular configuration assuming equal probability of placement. However, it was shown by Janssen¹⁶ based on compilation of earlier diode laser and mass-spectroscopic data of ozone isotopologues,^{17,37,38} that this ratio is not 2.00 but changes from 1.99 to 2.14 in consort with the enrichment in ^{18}O (bulk) varying from 47‰ to 156‰. The enrichment in this case is defined relative to the expected isotope ratio if the distribution is statistical and, as mentioned above, comprises non-fractionating arrangement of the atomic oxygen pool. That is, if the isotope ratio in the oxygen reservoir is $g = ^{18}\text{O}/^{16}\text{O}$ the ratio expected in molecular O_2 ($^{16}\text{O}^{18}\text{O}/^{16}\text{O}^{16}\text{O}$) is $2g$ and the ratio expected in bulk O_3 is $3g$ with ratio $2g$ in asymmetric type ($^{16}\text{O}^{16}\text{O}^{18}\text{O}/^{16}\text{O}^{16}\text{O}^{16}\text{O}$) and ratio g in symmetric type ($^{16}\text{O}^{18}\text{O}^{16}\text{O}/^{16}\text{O}^{16}\text{O}^{16}\text{O}$) molecule. The spectroscopic results show that the ratio in ozone is much higher than $3g$ and, moreover, the corresponding increases in $\delta^{18}\text{O}(\text{s})$ and $\delta^{18}\text{O}(\text{as})$ are not equal (s and as denote symmetric and asymmetric, respectively). As shown by Janssen¹⁶ the concentration ratio r_{50} is related to the enrichments in $^{18}\text{O}/^{16}\text{O}$ as follows: $r_{50} = 2^* [1000 + \delta^{18}\text{O}(\text{as})]/[1000 + \delta^{18}\text{O}(\text{s})]$. Janssen's analysis¹⁶ made it clear that the two ozone species are not only enriched individually but also the enrichment in asymmetric species is higher when the bulk enrichment is more than 60‰ and lower when the bulk enrichment is less. It seems that the heavy isotope content (say $^{18}\text{O}/^{16}\text{O}$) gets distributed among the asymmetric and symmetric types in a varying fashion. Since transfer of heavy isotopes from ozone to other atmospheric species (such as various NO_x species or nitrate) takes place during oxidation by ozone the site specific distribution of heavy isotopes in ozone molecule must be known to understand and model this transfer. Such information is also useful to infer changes in oxidation chemistry in the modern atmosphere^{26,28,31} or in ancient atmosphere through ice core nitrate as a proxy.^{1,21}

The internal isotopic distribution in ozone has been studied in more detail by Bhattacharya *et al.*⁷ who used a simple oxidation reaction where only one of the base atoms of ozone participates. By analyzing the reactants and products of the reaction, namely, the initial ozone (O_3) and the left-over O_2 they deduced the isotopomer ratios of asymmetric and symmetric heavy ozone species. Subsequently, similar studies have been carried out using three other reaction schemes,^{5,27,34} all yielding equivalent information. The present paper is a re-analysis of all these data which points to a new feature in the internal isotope distribution of ozone.

The paper is arranged as follows. We first give an overview of the earlier studies on ozone and describe our experiments briefly. Then we discuss the Hathorn-Gao-Marcus (HGM) model prediction in relation to the internal isotopic anomaly. Next, we give a summary of the results obtained in

our four earlier experiments and show that there is a deviation from the model prediction. A Chemical kinetic simulation is carried out next to derive rate constant ratios as function of pressure which would reproduce the observed data. Possible explanation of the deviation is then given in terms of dynamics of ozone formation and a speculation.

II. AN OVERVIEW OF THE EARLIER STUDIES ON THE INTERNAL ISOTOPE ANOMALY OF OZONE

In a pioneering effort, Janssen and Tuzson¹⁷ and Tuzson and Janssen³⁸ carried out TDLAS measurement to decipher internal distribution of heavy isotopes in ozone. Tuzson³⁷ also estimated the relative rate coefficient for both ^{18}O and ^{17}O species using the same technique. However, his result on symmetric ^{18}O species did not agree with the compilation of Janssen¹⁶ presumably due to large uncertainty in the line strengths. Nevertheless, his studies could estimate site specific enrichments in an adopted relative scale. The obtained values (in ‰) are as follows, for Mass 50: $\delta^{50}_{\text{as}} = 247.4 \pm 3.2$ and $\delta^{50}_{\text{s}} = 53.1 \pm 5.4$; and for mass 49: $\delta^{49}_{\text{as}} = 198.9 \pm 2.5$ and $\delta^{49}_{\text{s}} = 28.3 \pm 2.8$ where subscripts as and s denote the asymmetric and symmetric position, respectively. If we take these numbers as true absolute enrichments (mass 50 representing ^{18}O and mass 49 representing ^{17}O) in the sense discussed before, the $\Delta^{17}\text{O}(\text{as}) = 71.2 \pm 3.00$ and $\Delta^{17}\text{O}(\text{s}) = 0.90 \pm 3.95$. We note that these data show a small mass independent component in the symmetric position, albeit with large error.

In our work we adopted a different strategy. It is known that in the ground state the three atoms of ozone are located in three potential energy wells.⁴ The two base atoms are equivalent in the strength of their single bond with the apex atom which is less than that of the double bond of the apex atom with the two base atoms. It is therefore expected that in any chemical reaction involving ozone the base atoms would take part with higher probability. We assumed this probability to be 100% for certain specific reactions. For example, it was shown to be true by model calculations in case of reaction of ozone with nitrite ions in aqueous phase.²³ If this is so, one can analyze the isotopic composition of the O_2 molecule resulting from such reactions. Since the O_2 inherits one isotope from the base position and the other from the apex position one can, in principle, calculate the abundances (or isotope ratio) of ozone with the heavy isotope (X) located in the apex or symmetric position ($^{16}\text{OX}^{16}\text{O}$ type) as well as in the base or asymmetric position ($^{16}\text{O}^{16}\text{OX}$ type). For example, one can write the following mass balance equations for initial bulk O_3 and the O_2 produced by the reaction: $\text{O}_3 + \text{A} \rightarrow \text{O}_2 + \text{OA}$ (where A is the reaction partner):

$$3^*\delta\text{O}_3(\text{bulk}) = 2^*\delta(\text{as}) + \delta(\text{s}), \quad (2)$$

$$2^*\delta\text{O}_2(\text{produced}) = \delta(\text{as}) + \delta(\text{s}) + \varepsilon, \quad (3)$$

$$\delta(\text{OA}) = \delta(\text{as}) - \varepsilon, \quad (4)$$

where $\delta(\text{as})$ and $\delta(\text{s})$ express the two positional enrichments and ε is a kinetic fractionation constant in the above reaction.

Since ε is not known *a priori* we cannot determine $\delta(\text{as})$ and $\delta(\text{s})$. It is possible that one can estimate ε in certain cases and get around this problem.

However, if we are not interested in the individual positional enrichments in ^{17}O or ^{18}O but only in the magnitude of mass independence $\Delta^{17}\text{O}$ (as defined before) we can eliminate ε in some cases. For example, in most cases of oxidizing reaction we expect the fractionation ε to obey a mass dependent relation. This is implicitly assumed in several recent studies involving chemical kinetic modelling.^{7,33} It is also proved specifically for oxidation of silver and copper. Oxidation of silver metal by mass dependently fractionated ozone (formed by electrolysis) was studied by Bhattacharya *et al.*⁶ who found that the product silver oxide was depleted relative to the bulk ozone by 4.2‰ in ^{17}O and by 8.3‰ in ^{18}O on average giving a fractionation factor ratio of 0.51. We have recently conducted measurement of the kinetic fractionation associated with the reaction of oxygen with hot (270 °C) copper and found that the product copper oxide is depleted in heavy isotopes relative to the oxygen. Treating the oxidation as a Rayleigh process the two isotopic fractionations (ε^{17} and ε^{18}) are found to be related by $\varepsilon^{17} = 0.515 \cdot \varepsilon^{18}$. Based on these studies we can assume that for the reactions under consideration in the present work: $\varepsilon^{17} = 0.52 \cdot \varepsilon^{18}$. Therefore, in terms of $\Delta^{17}\text{O}$ Eqs. (2), (3), and (4) can be written as (using silver-ozone reaction case as example):

$$3 \cdot \Delta^{17}\text{O}(\text{bulk}) = 2 \cdot \Delta^{17}\text{O}(\text{as}) + \Delta^{17}\text{O}(\text{s}), \quad (5)$$

$$2 \cdot \Delta^{17}\text{O}(\text{O}_2) = \Delta^{17}\text{O}(\text{as}) + \Delta^{17}\text{O}(\text{s}), \quad (6)$$

$$\Delta^{17}\text{O}(\text{Ag}_2\text{O}) = \Delta^{17}\text{O}(\text{as}). \quad (7)$$

Using these equations we can obtain robust information on $\Delta^{17}\text{O}$ values of the two types (symmetric and asymmetric) of ozone.

III. BRIEF DESCRIPTION OF THE EXPERIMENTS

As mentioned, we carried out four experiments in three laboratories (Physical Research Laboratory, India; Laboratoire de Glaciologie et Géophysique de l'Environnement, France; and Purdue University, USA) and presented the data in four publications: Bhattacharya *et al.*,⁷ Savarino *et al.*,³⁴ Michalski and Bhattacharya,²⁷ and Berhanu *et al.*⁵ All these experiments deal with reactions of the type $\text{O}_3 + \text{A} \rightarrow \text{O}_2 + \text{OA}$ where A represents the following components: Silver metal foil, NO (Gas), NO_2^- (aqueous phase ionic species), and NO_2 (Gas phase). In these studies a diverse range of ozone samples with variable enrichments were obtained by suitable combination of pressure and temperature of the discharge/photolysis chamber. For details of the four experiments and the analyses of the results obtained the original papers should be referred but for clarity the salient points of the experiments are described below.

In brief, the initial oxygen pressure was varied from about 8 Torr to 100 Torr and the temperature from -196°C to about 90°C .³⁴ This variation allowed us to obtain ozone enrichments from 10‰ to 120‰ ($\delta^{18}\text{O}$). We believe that the internal

isotope distribution correlate with the bulk enrichment and it does not matter what temperature-pressure condition is used to make ozone with a certain bulk enrichment. For example, in the study of Bhattacharya *et al.*⁷ ozone formed by photolysis and discharge (using different P, T conditions) lead to similar internal isotopic distribution. It is to be noted that in case of discharge the temperature and pressure are both ill-defined as discharge is an out of equilibrium situation. In this case T and P mean the values measured when the discharge is temporarily turned off. We should mention here that in all these four experiments the chamber used for making ozone had small surface to volume ratio to minimize the effect of surface formation of ozone. This precaution was necessary because Janssen and Tuzson¹⁸ have shown that ozone formed on glass surface by discharge at low pressures can have both mass independent and mass dependent component depending on the pressure and vessel size. Similarly, ozone formed by electrolysis on platinum surface follows pure mass dependent fractionation in both apex and base positions.⁶ Therefore, a contribution from surface formed ozone may influence the site specific isotope distribution and would not allow a precise comparison of the experimental results with the gas phase model.

In all cases, the produced ozone was collected by liquid nitrogen cooled trap. This was split into a small aliquot for determining the bulk initial composition (after converting ozone to O_2) and a larger fraction to react with (1) silver foil, (2) NO in gas phase, (3) NO_2^- ionic species in liquid phase, and (4) NO_2 in gas phase, respectively. The product oxygen gas (or in case of silver foil experiment the oxygen released from Ag_2O by heating) was collected and analyzed. From these two sets of $\delta^{17}\text{O}$ and $\delta^{18}\text{O}$ numbers (one for O_3 and the other for O_2) we calculated the $\Delta^{17}\text{O}$ for ozone and oxygen. We then used Eqs. (5), (6), and (7) to calculate $\Delta^{17}\text{O}(\text{as})$ and $\Delta^{17}\text{O}(\text{s})$; these values are given in Table I–IV, respectively for the four experiments mentioned above. Typical errors associated with oxygen isotope analysis in these experiments are 0.1‰ for $\delta^{18}\text{O}$ and 0.2‰ for $\delta^{17}\text{O}$. The error for $\Delta^{17}\text{O}$ is less (estimated to be about 0.1‰) since the two errors in $\delta^{18}\text{O}$ and $\delta^{17}\text{O}$ are often correlated in a mass dependent way.

In the present work we pool up information from these four experiments in terms of $\Delta^{17}\text{O}$ of initial bulk ozone and that of the produced O_2 gas (or the product OA in case of silver metal) and analyze them in the light of prediction based on the HGM model.

IV. THE HATHORN-GAO-MARCUS (HGM) MODEL PREDICTION

The Hathorn-Gao-Marcus (HGM) model papers^{8–10,12,13} propose a semi-empirical scheme to calculate the anomalous isotopic enrichment in ozone based on the idea that asymmetric isotopomers of ozone (such as $^{16}\text{O}^{16}\text{O}^{17}\text{O}$ and $^{16}\text{O}^{16}\text{O}^{18}\text{O}$) are formed preferentially from the transition state during the collision of isotopic species of oxygen atom and molecule. It is known that ozone forms from a small fraction of the total number of collision complexes as most of them either re-dissociate or undergo isotope exchange. HGM assumes that the asymmetric molecules have more rovibronic couplings

TABLE I. Isotopic data of ozone and silver oxide used for determining anomaly of asymmetric (XXZ type) and symmetric (XZX type) ozone expressed in ‰ relative to the starting oxygen composition.

Sample no.	Ozone			Silver oxide			Ozone asymm	Ozone symm
	$\delta^{18}\text{O}$	$\delta^{17}\text{O}$	$\Delta^{17}\text{O}$	$\delta^{18}\text{O}$	$\delta^{17}\text{O}$	$\Delta^{17}\text{O}$	$\Delta^{17}\text{O}$	$\Delta^{17}\text{O}$
P-1	13.7	16.6	9.5	-1.4	22.4	23.1	23.1	-17.8
P-2	18.3	21.7	12.2	4.6	26.4	24.0	24.0	-11.5
P-3	22	23.9	12.5	13.9	35.8	28.6	28.6	-19.8
P-4	33.6	30.4	12.9	28.4	43.3	28.5	28.5	-18.3
P-5	34.5	35.1	17.2	13.6	34.5	27.4	27.4	-3.4
P-6	40.8	37.8	16.6	31.8	49.3	32.8	32.8	-15.8
P-7	43.1	40.5	18.1	39.3	50.3	29.9	29.9	-5.5
P-8	44.4	41	17.9	38.5	54.7	34.7	34.7	-15.6
P-9	46.9	44.1	19.7	43.2	59.3	36.8	36.8	-14.5
P-10	47.2	41.8	17.3	45.5	59.1	35.4	35.4	-19.1
P-11	49.3	45.1	19.5	31.2	49.9	33.7	33.7	-9.0
P-12	51.1	43.3	16.7	25.3	40.9	27.7	27.7	-5.3
P-13	51.3	43.4	16.7	31.6	43.5	27.1	27.1	-4.0
P-14	51.9	47.6	20.6	43.9	56.9	34.1	34.1	-6.3
P-15	54.7	51.3	22.9	44.8	55.2	31.9	31.9	4.8
P-16	56.1	48.6	19.4	35.2	51.7	33.4	33.4	-8.5
P-17	59	53	22.3	46	58.1	34.2	34.2	-1.4
P-18	62.6	50.8	18.2	46.1	54.9	30.9	30.9	-7.1
P-19	67.4	63.7	28.7	71.2	83.1	46.1	46.1	-6.2
P-20	68.7	64.5	28.8	68.3	81.7	46.2	46.2	-6.0
P-21	69.1	63.9	28.0	71.5	83.3	46.1	46.1	-8.3
P-22	71.3	66.4	29.3	77.1	87.3	47.2	47.2	-6.4
P-23	72.5	71	33.3	71.8	81.4	44.1	44.1	11.8
P-24	77.3	70.3	30.1	76.3	87.4	47.7	47.7	-5.1
P-25	78	70.5	29.9	76.3	86.4	46.7	46.7	-3.6
P-26	81.4	76.9	34.6	87.3	93.9	48.5	48.5	6.7
P-27	89.8	83.5	36.8	99.5	103.3	51.6	51.6	7.3
P-28	91.8	88.1	40.4	91.8	101.9	54.2	54.2	12.8
P-29	97.1	92.6	42.1	89.8	99.6	52.9	52.9	20.5
P-30	101.8	87.2	34.3	90.2	94.6	47.7	47.7	7.4
P-31	102	95.6	42.6	118.6	121.6	59.9	59.9	7.8
P-32	102.4	96.3	43.1	94.6	104.4	55.2	55.2	18.7
P-33	104.3	95.9	41.7	100.5	106.6	54.3	54.3	16.3
P-34	104.7	98.2	43.8	100.7	108.8	56.4	56.4	18.4
P-35	111.6	104.3	46.3	120.8	126.9	64.1	64.1	10.6
P-36	112.8	102	43.3	108.8	115.4	58.8	58.8	12.4
P-37	115.6	106.3	46.2	113.9	122.7	63.5	63.5	11.6
L-1	10.7	11.7	6.1	-1.4	17.4	18.1	18.1	-17.8
L-2	20.7	21.7	10.9	5	25.8	23.2	23.2	-13.6
L-3	28.1	29	14.4	19.4	36.6	26.5	26.5	-9.9
L-4	39.4	40.4	19.9	26	45.5	32.0	32.0	-4.2
L-5	45.9	45.4	21.5	35.4	52.1	33.7	33.7	-2.8
L-6	52.3	51.6	24.4	42.1	58.2	36.3	36.3	0.6
L-7	53.1	51.3	23.7	38.7	56.1	36.0	36.0	-0.9
L-8	60.7	57.1	25.5	58.2	66.3	36.0	36.0	4.5
L-9	64.4	60.4	26.9	56.7	70.4	40.9	40.9	-1.1
L-10	76.4	70.4	30.7	72.6	82.2	44.4	44.4	3.1
L-11	83.9	75.4	31.8	76.5	85.9	46.1	46.1	3.1
L-12	84.1	76.6	32.9	81	88.5	46.4	46.4	5.8
L-13	86.4	76.8	31.9	88	88.2	42.4	42.4	10.7
L-14	98.2	84.5	33.4	88.1	93.4	47.6	47.6	5.1
L-15	106.2	91.8	36.6	100.8	104.6	52.2	52.2	5.4

compared to the symmetric molecules, which implies a longer life-time for the asymmetric complexes resulting in a higher rate of stabilization for them.⁹ It follows that as long as symmetry is considered to be the principal driving mechanism, the

isotopic anomaly (expressed by the parameter $\Delta^{17}\text{O}$) in ozone would be exclusively associated with asymmetric molecules. This means that $\Delta^{17}\text{O}(\text{s})$ is zero. In other word, the apex atom only dilutes the total anomaly. The anomaly in the asymmetric

TABLE II. Isotopic data of ozone and product oxygen used for determining asymmetric (XXZ type) and symmetric (XZX type) ozone anomaly expressed in ‰ relative to the starting oxygen composition based on NO + O₃ reaction. The probability of central atom reaction is denoted by p (see text for details).

Sample no.	Ozone			Product oxygen			p = 0.0		p = 0.082	
							Ozone asymm	Ozone symm	Ozone asymm	Ozone symm
	$\delta^{18}\text{O}$	$\delta^{17}\text{O}$	$\Delta^{17}\text{O}$	$\delta^{18}\text{O}$	$\delta^{17}\text{O}$	$\Delta^{17}\text{O}$	$\Delta^{17}\text{O}$	$\Delta^{17}\text{O}$	$\Delta^{17}\text{O}$	$\Delta^{17}\text{O}$
1	-6.4	-2.6	0.7	9.0	2.3	-2.4	6.8	-11.5	8.8	-15.5
2	7.1	8.8	5.1	17.5	10.0	0.9	13.5	-11.8	16.2	-17.3
3	12.2	13.0	6.7	21.8	13.4	2.1	15.8	-11.6	18.8	-17.6
4	13.1	16.5	9.7	16.5	12.4	3.8	21.5	-14.0	25.3	-21.7
5	27.1	28.9	14.8	32.5	26.0	9.1	26.1	-7.9	29.8	-15.3
6	30.5	29.1	13.3	36.5	26.7	7.7	24.4	-8.9	28.0	-16.1
7	43.1	38.9	16.5	46.4	33.6	9.5	30.5	-11.6	35.1	-20.8
8	48.7	44.8	19.4	49.7	40.3	14.4	29.5	-0.6	32.7	-7.1
9	64.9	59.4	25.7	64.9	50.8	17.1	42.8	-8.6	48.4	-19.8
10	66.9	59.7	24.9	66.8	52.7	18.0	38.8	-2.9	43.4	-12.0
11	69.8	65.1	28.8	70.6	57.3	20.6	45.4	-4.2	50.8	-15.0
12	82.9	74.2	31.1	82.9	66.5	23.4	46.5	0.4	51.5	-9.6
13	97.0	86.0	35.6	94.9	76.7	27.3	52.1	2.5	57.5	-8.2
14	111.9	94.3	36.1	109.0	84.7	28.0	52.3	3.7	57.6	-6.8

TABLE III. Isotopic data of ozone and product oxygen used for determining asymmetric (XXZ type) and symmetric (XZX type) ozone anomaly expressed in ‰ relative to the starting oxygen composition based on NO₂ + O₃ reaction.

Sample	Ozone			Product oxygen			Ozone asymm	Ozone symm
	$\delta^{18}\text{O}$	$\delta^{17}\text{O}$	$\Delta^{17}\text{O}$	$\delta^{18}\text{O}$	$\delta^{17}\text{O}$	$\Delta^{17}\text{O}$	$\Delta^{17}\text{O}$	$\Delta^{17}\text{O}$
Purdue-1	60.8	47.9	16.3	52.1	36.6	9.6	29.7	-10.6
Purdue-2	71.0	55.6	18.7	63.5	46.3	13.2	29.6	-3.1
Purdue-3	73.9	57.4	19.0	62.6	44.0	11.4	34.2	-11.3
Purdue-4	59.9	50.5	19.4	53.2	41.2	13.6	31.1	-3.9
Purdue-5	76.3	64.0	24.3	68.5	54.3	18.7	35.5	1.9
Purdue-6	87.0	69.7	24.4	77.9	58.8	18.3	36.7	-0.2
Purdue-7	94.4	74.0	24.9	82.4	59.7	16.9	41.1	-7.4
Purdue-8	91.6	73.2	25.6	81.3	60.2	17.9	41.0	-5.2
Purdue-9	86.4	71.9	27.0	76.9	60.8	20.8	39.4	2.2
Purdue-10	98.0	80.6	29.7	87.5	68.2	22.7	43.8	1.5
Purdue-11	95.3	79.3	29.7	84.8	67.2	23.1	42.9	3.3
Purdue-12	111.0	89.1	31.4	100.4	76.1	23.9	46.5	1.2
Purdue-13	110.0	89.9	32.7	97.3	74.5	23.9	50.2	-2.4
Purdue-14	106.5	88.2	32.8	95.4	75.0	25.4	47.5	3.4
Purdue-15	105.9	87.9	32.8	90.7	71.4	24.3	49.9	-1.4
Purdue-16	111.4	91.0	33.1	103.6	81.3	27.4	44.4	10.5
Purdue-17	116.5	93.8	33.2	107.9	82.7	26.6	46.5	6.7
Purdue-18	115.0	93.6	33.8	106.6	82.2	26.7	47.8	5.6
Purdue-19	114.3	93.6	34.1	102.6	79.4	26.0	50.4	1.6
Purdue-20	113.4	93.2	34.2	102.0	78.5	25.5	51.7	-0.8
Purdue-21	115.4	94.4	34.4	101.7	78.5	25.7	51.7	-0.4
Purdue-22	117.4	95.4	34.4	107.8	83.7	27.6	47.9	7.4
Purdue-23	124.4	99.6	34.9	113.7	87.9	28.8	47.1	10.5
Purdue-24	124.6	99.8	35.0	113.0	87.3	28.5	48.1	9.0
Purdue-25	117.2	96.4	35.4	108.0	85.2	29.0	48.2	9.9
Purdue-26	125.7	101.1	35.7	114.5	87.5	28.0	51.2	4.8
Purdue-27	133.3	108.1	38.8	125.2	96.0	30.9	54.7	7.1
Purdue-28	144.2	114.8	39.9	138.5	105.7	33.7	52.1	15.4
Purdue-29	151.7	120.5	41.6	141.0	108.4	35.1	54.6	15.5
Purdue-30	164.3	128.5	43.1	150.9	113.3	34.8	59.6	10.1
Purdue-31	165.8	130.0	43.8	151.1	113.3	34.8	61.9	7.6
Purdue-32	177.0	136.0	43.9	159.6	119.7	36.7	58.4	15.0
Purdue-33	161.0	127.7	44.0	146.4	111.5	35.3	61.3	9.4

TABLE IV. Isotopic data of ozone and product oxygen used for determining asymmetric (XXZ type) and symmetric (XZX type) ozone anomaly expressed in ‰ relative to the starting oxygen composition based on NO₂ (gas) + O₃ reaction.

Sample no.	Ozone			Product oxygen			Ozone asymm	Ozone symm
	$\delta^{18}\text{O}$	$\delta^{17}\text{O}$	$\Delta^{17}\text{O}$	$\delta^{18}\text{O}$	$\delta^{17}\text{O}$	$\Delta^{17}\text{O}$	$\Delta^{17}\text{O}$	$\Delta^{17}\text{O}$
1	7.5	10.1	6.2	10.4	5.3	-0.2	18.8	-19.1
2	8.7	13.7	9.2	17.5	12.1	3.0	21.4	-15.3
3	11.2	15.4	9.6	24.3	15.8	3.2	22.3	-16.0
4	24.5	22.5	9.8	32.0	18.4	1.9	25.6	-21.8
5	20.7	20.8	10.0	34.7	22.9	4.8	20.3	-10.6
6	17.4	20.7	11.6	29.7	20.8	5.4	24.2	-13.5
7	35.9	32.5	13.9	38.6	28.8	8.7	24.2	-6.8
8	44.9	40.9	17.6	39.8	32.5	11.7	29.4	-6.1
9	43.9	40.5	17.6	43.8	34.4	11.5	30.0	-7.0
10	34.3	38.3	20.5	44.8	37.3	13.8	33.8	-6.1
11	33.1	37.7	20.5	45.7	36.6	12.7	36.0	-10.5
12	52.6	49.0	21.7	63.8	49.9	16.6	31.9	1.2
13	53.8	50.1	22.1	57.2	46.4	16.4	33.5	-0.7
14	47.7	48.5	23.7	56.9	46.7	16.9	37.4	-3.6
15	43.6	46.7	24.0	41.8	37.6	15.6	40.7	-9.4
16	71.0	65.1	28.2	74.9	61.1	21.7	41.2	2.3
17	55.6	57.1	28.2	63.7	54.4	20.8	43.1	-1.5
18	73.4	69.0	30.8	79.0	65.3	23.7	45.0	2.4
19	86.6	77.9	32.9	93.1	72.8	24.0	50.6	-2.6
20	89.8	81.6	34.9	99.5	77.6	25.4	53.9	-3.2
21	107.0	92.3	36.6	111.9	84.9	26.3	57.2	-4.6
22	107.1	93.2	37.5	108.0	84.2	27.6	57.5	-2.3
23	106.6	93.2	37.8	111.0	85.4	27.2	59.0	-4.6
24	103.3	91.9	38.2	109.1	85.4	28.1	58.3	-2.2
25	102.5	92.2	38.9	98.9	80.5	28.4	59.8	-3.0
26	107.8	95.5	39.5	111.8	87.6	28.9	60.7	-3.0
27	110.8	98.0	40.4	116.4	92.2	30.9	59.5	2.4
28	106.0	96.7	41.6	111.3	90.2	31.4	62.0	0.9

position must then obey (from Eq. (5)):

$$\Delta^{17}\text{O}(\text{as}) = 1.5 * \Delta^{17}\text{O}(\text{bulk}). \quad (8)$$

We call this simply as *1.5 rule* for further discussion. As mentioned before, the δ -values are expressed relative to the corresponding symmetric or asymmetric entities assuming that they form by a non-fractionating statistical distribution of the ¹⁶O, ¹⁷O and ¹⁸O isotopes as available in the hypothetical atomic reservoir made from the parent oxygen gas.

This prediction has been independently checked now by calculating the isotopic enrichment of the four heavy ozone species (¹⁶O¹⁷O¹⁶O, ¹⁶O¹⁸O¹⁶O, ¹⁶O¹⁶O¹⁷O, and ¹⁶O¹⁶O¹⁸O) using the HGM model. The isotopic composition of ozone has negative pressure dependence. The pressure dependence is weak at pressures less than 100 mbar but becomes significant at a higher pressure. For example, $\delta^{50}\text{O}_3$ decreases by ~30‰ at pressures from ~100 to 1000 mbar. The pressure dependent calculation of each isotope-variant rate coefficient was done by parameterizing them following the semi-analytic approach given in Gao and Marcus⁸ and further outlined in Liang *et al.*²² We fit the fractionation factor ε of each rate coefficient at a given temperature by

$$\varepsilon = \varepsilon_0 / (1 + P/P_{1/2}), \quad (9)$$

where P is the pressure of interest and P_{1/2} is the pressure at which ε takes one-half of the value of its low-pressure limit ε_0 . Both P_{1/2} and ε_0 are isotope-variant and temperature-dependent. The values of the latter are presented by Liang *et al.*²² The functional dependence of P_{1/2} is rather complicated but was derived by fitting experimental enrichment¹¹ values. For example, the effective P_{1/2} of $\delta^{50}\text{O}_3$ (¹⁶O¹⁶O¹⁸O + ¹⁶O¹⁸O¹⁶O) at 300 K is 2.6 bars. The derived values agree with that given in Gao and Marcus.¹⁰ Regarding the T-dependence the important point to note is that the η parameter and ΔE are taken to be the same as those suggested by Gao and Marcus;⁹ that is $\eta = 1.13$ at 140 K and 1.18 at 300 K and linear interpolation was used between these two temperatures. ΔE is assumed to be 260 cm⁻¹ (constant). The η values are taken to be the same for two heavy symmetrical species: ¹⁶O¹⁷O¹⁶O and ¹⁶O¹⁸O¹⁶O since they have the same symmetry.

For the range of $\Delta^{17}\text{O}(\text{bulk})$ values from 32‰ to 50‰ (or corresponding bulk $\delta^{18}\text{O}$ values from 88‰ to 130‰) the ratio $\Delta^{17}\text{O}(\text{as})/\Delta^{17}\text{O}(\text{bulk})$ varies over a narrow range of 1.47–1.52 (Figure 1). For $\delta^{18}\text{O}(\text{bulk})$ values lower than 88‰ (corresponding to pressures higher than about 700 mbar) the calculations were not done as the parameterization could not be done over this range. Therefore, both from the basic hypothesis of the HGM model as well as simple numerical

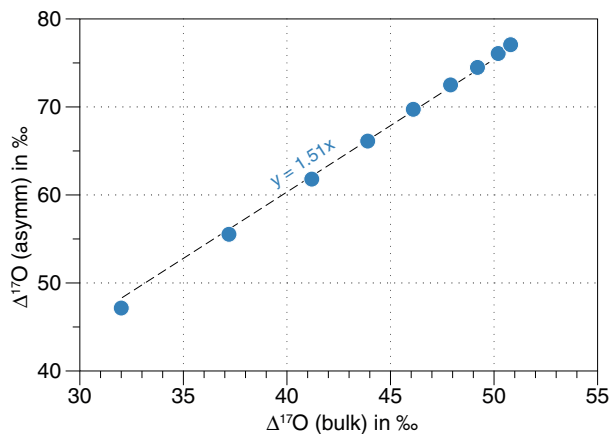


FIG. 1. Results of numerical calculation based on Gao and Marcus⁸ scheme showing a linear relationship between $\Delta^{17}\text{O}$ (Asymmetric) and $\Delta^{17}\text{O}$ (bulk) of ozone (relative to starting oxygen) showing a slope of 1.51 close to the value 1.5 expected based on HGM model of ozone isotopic enrichment (see text).

calculations based on their model (albeit over a limited range) we expect the *1.5 rule* to be valid.

V. HGM MODEL AND EXPERIMENTAL DATA (WITH SOME CAVEATS)

For the reaction schemes discussed in Sec. II where O_2 is produced by oxidative removal of one base atom we get,

$$\Delta^{17}\text{O}(\text{as}) = 2 * \Delta^{17}\text{O}(\text{O}_2). \quad (10)$$

And for silver-ozone reaction case if oxygen in silver oxide itself is analyzed by heating the Ag_2O and getting the oxygen out, we have (as given before and rewritten here):

$$\Delta^{17}\text{O}(\text{as}) = \Delta^{17}\text{O}(\text{Ag}_2\text{O}). \quad (7')$$

This allows us to test the prediction of the HGM model since we can determine $\Delta^{17}\text{O}(\text{as})$ from the $\Delta^{17}\text{O}(\text{O}_2)$ data or the $\Delta^{17}\text{O}(\text{Ag}_2\text{O})$ data. We can then plot $\Delta^{17}\text{O}(\text{as})$ against $\Delta^{17}\text{O}(\text{bulk})$ to check if a slope value of 1.5 is obtained. For clarity we should mention that although the four experiments were formally similar, each had its own characteristic. For silver-ozone reaction experiment we found it proper to use the resultant silver oxide rather than the oxygen. The silver oxide was heated to release all of its oxygen leaving clean silver foil back at its original state. The reason for using Ag_2O is in this case only a small part of ozone took part in reaction whereas the rest was catalytically decomposed thus contaminating the oxygen fraction produced by the reaction. For NO-Ozone reaction our analysis showed that the central atom possibly took part in about 8% of cases (central atom reaction probability $p = 0.082$) which needed to be accounted for. For this one had to use an empirical relationship connecting the asymmetric ozone enrichment to the bulk one which was based on the earlier published silver-ozone reaction data. The details of how it was done are explained in Savarino *et al.*³⁴ In this context, it is to be noted that if we assume a relationship between $\Delta^{17}\text{O}(\text{as})$ versus $\Delta^{17}\text{O}(\text{bulk})$ we can obtain p , the probability of central atom reaction. On the other hand, if we assume $p = 0$ we can obtain the required relationship.

In the absence of any other experimental input (such as, for example, spectroscopic data) this ambiguity is unavoidable. We present both cases ($p = 0$ and $p = 0.082$) for the NO-ozone reaction in Table II. It is seen that as p increases from 0 to 0.082 the $\Delta^{17}\text{O}(\text{as})$ increases by 2‰–5‰ and correspondingly $\Delta^{17}\text{O}(\text{s})$ decreases by 4‰–10‰. For $\text{NO}_2^- + \text{ozone}$ (in aqueous phase), we are on a firm ground to assume $p = 0$ based on the independent study by Liu *et al.*²³ mentioned before. For NO_2 gas ozone oxidation we assume again that the reaction is due to the base atoms alone without any contribution from the apex atom. Notwithstanding these caveats all four experiments can be used to determine the asymmetric and symmetric position anomaly. We should mention here that under the assumption of $p = 0$ all four different experiments involving solid, liquid and gas phase reactants yield very similar relationship between $\Delta^{17}\text{O}(\text{as})$ and $\Delta^{17}\text{O}(\text{bulk})$ which provides an indirect support for the assumption that p is close to zero.

VI. DEVIATION FROM THE HGM MODEL PREDICTION

The basic data for the four experiments are summarized in the Table I–IV in the form of delta values of ozone and resultant oxygen along with derived $\Delta^{17}\text{O}$ values for the asymmetric and symmetric position. The $\delta^{18}\text{O}$ (or $\delta^{17}\text{O}$) values are linearly correlated with $\Delta^{17}\text{O}$ values as shown in Figure 2 for the combined data set pertaining to ozone-silver, ozone-NO, ozone- NO_2 (gas) reaction data and the best fit line (with 1σ error) is given by: $\delta^{18}\text{O} = 2.784 (\pm 0.072) * \Delta^{17}\text{O} - 8.205 (\pm 1.981)$. If this equation is used for predicting $\delta^{18}\text{O}$ value (as will be done later) from the measured $\Delta^{17}\text{O}$ value some uncertainty will be introduced by the spread of the data points. The absolute deviations of the data points from the fitted line range from 0.2‰ to 15.8‰ (with only 15 points deviating more than 10‰). The mean absolute deviation is 5.6‰ and this value can be taken to be the uncertainty of the

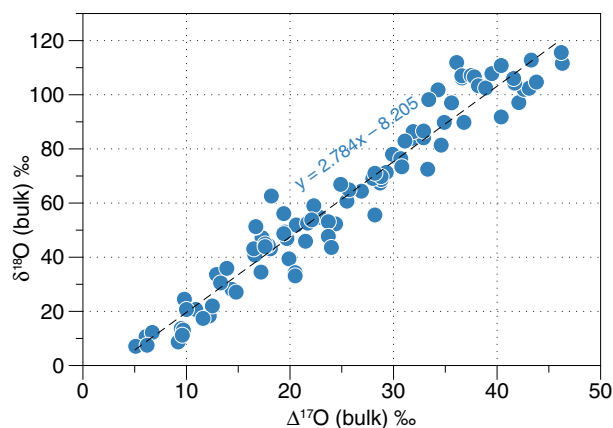


FIG. 2. A linear relationship between $\Delta^{17}\text{O}$ (bulk) and $\delta^{18}\text{O}(\text{bulk})$ observed in ozone samples prepared by Tesla discharge of oxygen. The δ -values are relative to tank oxygen expressed in ‰. The plot is based on three sets of experimental data obtained from: silver- O_3 , NO- O_3 , and NO_2 gas- O_3 reactions. The isotopes in these three experiments were analyzed using the same calibration and hence can be combined for deriving a common correlation line. The equation of the best fit line is: $y = 2.784 (\pm 0.072)x - 8.205 (\pm 1.981)$ where the errors are 1σ .

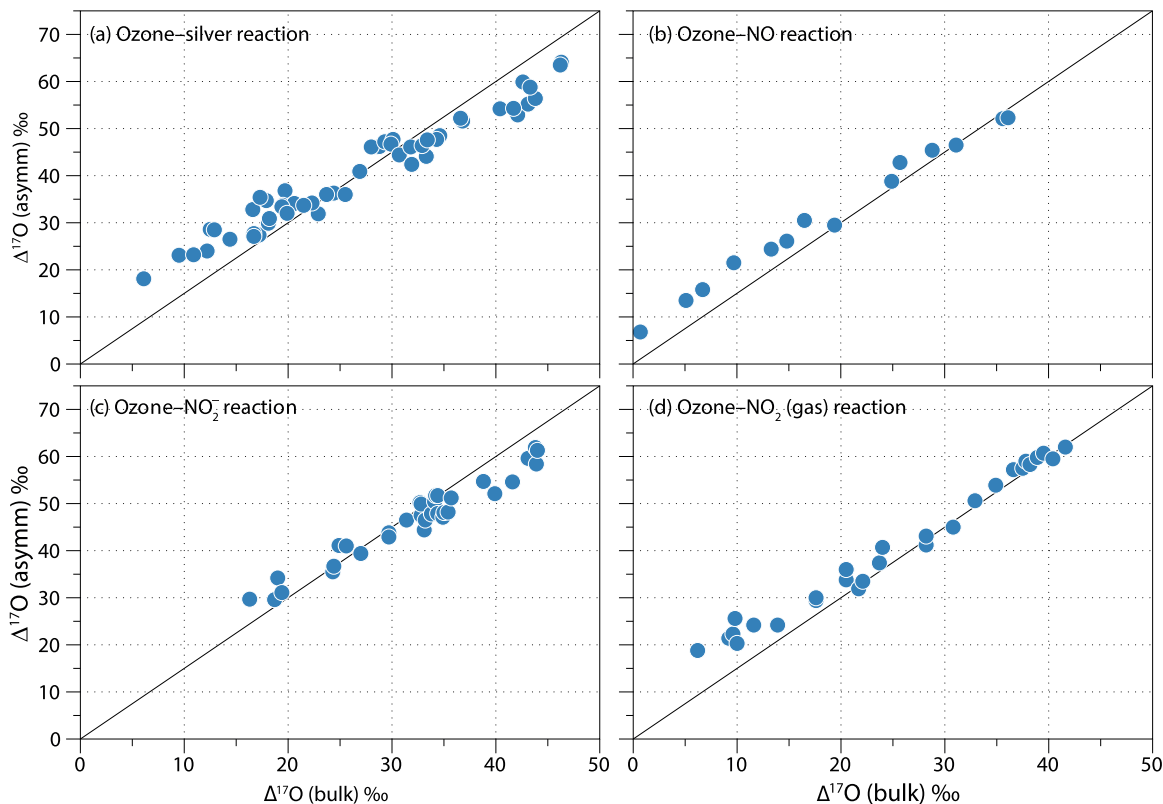


FIG. 3. Scatter diagram of data points showing linear pattern between $\Delta^{17}\text{O}(\text{asymmetric})$ and $\Delta^{17}\text{O}(\text{bulk})$ obtained from four experiments designed to determine the isotopic anomaly $[\delta^{17}\text{O} - 0.52\delta^{18}\text{O}]$ of ozone samples produced in Tesla discharge of oxygen gas. 3a, 3b, 3c and 3d refer to experiments based on Ozone–silver reaction, Ozone–NO reaction, Ozone– NO_2^- reaction, and Ozone– NO_2 (gas) reaction as described in Bhattacharya *et al.*,⁷ Savarino *et al.*,³⁴ Michalski and Bhattacharya,²⁷ and Berhanu *et al.*,⁵ respectively. The expected relation [1.5 rule] based on Hathorn-Gao-Marcus model is shown by the straight lines for comparison. The observed data points deviate slightly from the 1.5 rule in each case.

estimate in δ -value. Individual plots showing $\Delta^{17}\text{O}(\text{as})$ versus $\Delta^{17}\text{O}(\text{bulk})$ for the four cases are given in Figures 3(a)–3(d). In the same plots we also show the expected line based on the 1.5 rule [i.e., $\Delta^{17}\text{O}(\text{as}) = 1.5 \times \Delta^{17}\text{O}(\text{bulk})$]. It is quite clear that the distribution of the points deviate significantly from the 1.5 rule at the lowest and highest range of $\Delta^{17}\text{O}$ values. When all the data points are pooled together and plotted in a single diagram (Figure 4) the best fit line is given by: $\Delta^{17}\text{O}(\text{as}) = 1.14(\pm 0.02) \times \Delta^{17}\text{O}(\text{bulk}) + 10.43(\pm 0.60)$. This line intersects the 1.5 slope line at $\Delta^{17}\text{O}$ value of 30‰. Correspondingly, the plot of $\Delta^{17}\text{O}(\text{s})$ against $\Delta^{17}\text{O}(\text{bulk})$ deviates from zero value. The best fit line in this case has a slope $0.716(\pm 0.042)$ and intercept $-20.85(\pm 1.21)$. We note that if we restrict to the $\Delta^{17}\text{O}$ values within 20‰–40‰ range the 1.5 rule is reasonably valid and the HGM model prediction is correct. For values less than 20‰ the observed $\Delta^{17}\text{O}(\text{as})$ values are higher than the prediction and for values above 40‰ they are less. Since the bulk $\Delta^{17}\text{O}$ is composed of the asymmetric and symmetric $\Delta^{17}\text{O}$ values this would imply opposite behavior for the symmetric position. Though the deviation is not large (of the order of 5‰ at the two end points) it is significantly different from the “global” prediction of the HGM model, which should be valid over the whole range. The 1.5 rule arises out of a robust and simple consideration of symmetry, namely, the isotopic anomaly is entirely due to the effect of symmetry on the stabilization efficiency of the collision complex towards formation of the ozone molecule

and this difference in formation efficiency is independent of the heavy isotopic species (i.e., ^{17}O or ^{18}O). In terms of the η -parameter (the empirical number by which the state density of the symmetric transition complexes is reduced relative to the asymmetric ones) its value is taken to be the same for ^{17}O and ^{18}O species as emphasized by Marcus in his re-

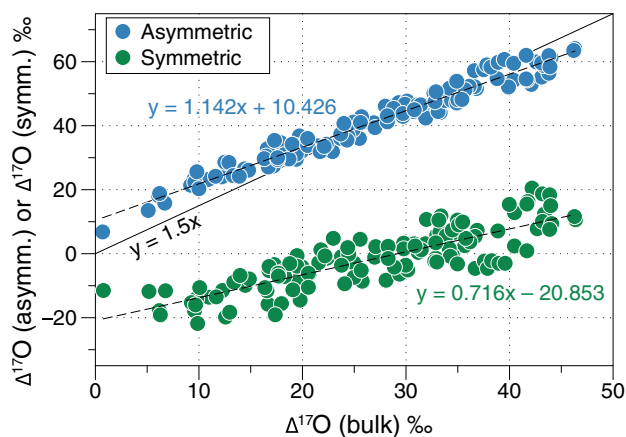


FIG. 4. $\Delta^{17}\text{O}(\text{Asymm.})$ (blue points) and $\Delta^{17}\text{O}(\text{Symm.})$ (green points) as function of $\Delta^{17}\text{O}(\text{bulk})$ based on four experiments whose data are shown in Figures 3(a)–3(d). The line with equation $1.142(\pm 0.021) \times \Delta^{17}\text{O}(\text{bulk}) + 10.426(\pm 0.60)$ refers to asymmetric species and the line with equation $0.716(\pm 0.042) \times \Delta^{17}\text{O}(\text{bulk}) - 20.85(\pm 1.21)$ refers to symmetric species. The line with slope 1.5 expected for $\Delta^{17}\text{O}(\text{Asymm.})$ from Hathorn-Gao-Marcus model is shown for comparison. Note the deviation of the observed points from the HGM model.

cent review:²⁴ “This property of a reduced number of coupling elements for symmetric systems is the same for all symmetrical isotopomers regardless of isotopic masses, since all have the same common symmetry property.” A clue to what could be the reason for the deviation can be found in a statement by Schinke *et al.*³⁵ that “the HGM model is valid for a strictly statistical ozone molecule but the apparently weak coupling between the three intramolecular modes imply that most of the wave functions in the vicinity of the dissociation threshold do not show the behavior typical for an irregular system.” We believe that our data provides evidence of a small but true departure from the irregular behavior of the ozone transition complex assumed in the HGM model for the P and T ranges under consideration. This is further explored in Secs. VIII and IX.

VII. CHEMICAL KINETICS SIMULATION AND CHANGES IN RATE CONSTANT RATIOS WITH P AND T

A. Model simulation

To understand the implications of the experimental data we need to investigate the kinetics of ozone formation based on an analysis of the chemical reactions occurring in the discharge chamber using a chemical kinetic simulator involving oxygen and ozone isotopomers. Even though the chemistry in a discharge chamber is quite complex due to the presence

of a variety of excited species and their reactions, a simple scheme of reactions should be applicable for simulating the isotopic composition of ozone. This is because the ozone formation in a Tesla discharge has been shown to be dominated by neutral O-atoms and O₂ molecules in their ground state.¹⁹ In addition, the ozone experiments by Bhattacharya *et al.*⁷ demonstrated that photolysis and discharge experiments lead to similar internal isotopic distribution. In their study, the UV photolysis of oxygen was done by varying pressure whereas the Tesla discharge was done by varying both pressure (P) and temperature (T). The internal distributions at the same enrichment level produced by the two processes were compared and found to be similar (see also Ref. 16).

We used a program named Kintecus (courtesy Ianni¹⁴ and accessed from www.kintecus.com) and modified it slightly to calculate the concentrations of four heavy isotopologues of ozone formed by reactions of O-atoms and O₂ molecules. We considered a total of 23 reactions (Table V) divided into four sets (number of reactions in bracket): set 1: O₂ dissociation (3), set 2: Isotope exchange between O-atom and O₂ molecule (4), set 3: O₃ formation (9), and set 4: O₃ dissociation (7). The last set is introduced to obtain a steady state in the ozone isotopologue composition and is expected to occur by the same discharge, which causes dissociation of O₂. We consider only the most abundant heavy isotopic species (having only one heavy isotope) for the reactions disregarding doubly substituted species. This causes some minor problem in obtaining

TABLE V. List of reactions along with the rate constants used in the Kintecus model for simulation of ozone production by discharge of oxygen. The choice of the rate constants is discussed in the text (see Secs. VII A–VII F). A factor of 0.5 is introduced when there are two channels for the same reactants. Units for the rate constants are: for dissociation (k1 and k4) s⁻¹; for two-body and three-body reactions (k2 and k3) cm³ s⁻¹ and cm⁶ s⁻¹, respectively. A, B, C, and D are the rate constant ratios to be found by fitting the δ -values of ozone and the corresponding isotope anomaly, $\Delta^{17}\text{O}$ (bulk) and $\Delta^{17}\text{O}(\text{as})$ for the two cases: (1) predicted by the HGM model and (2) present experimental data by trial and error method (see text).

Chemistry	Number	Reaction	Rate constant
Oxygen discharge	R(1a)	$^{16}\text{O}^{16}\text{O} \rightarrow ^{16}\text{O} + ^{16}\text{O}$	k1a = 2.5×10^{-3}
	R(1b)	$^{16}\text{O}^{18}\text{O} \rightarrow ^{16}\text{O} + ^{18}\text{O}$	k1b = k1a
	R(1c)	$^{16}\text{O}^{17}\text{O} \rightarrow ^{16}\text{O} + ^{17}\text{O}$	k1c = k1a
Exchange of O with O ₂	R(2a)	$^{18}\text{O} + ^{16}\text{O}^{16}\text{O} \rightarrow ^{16}\text{O} + ^{16}\text{O}^{18}\text{O}$	k2a = 2.90×10^{-12}
	R(2b)	$^{16}\text{O} + ^{16}\text{O}^{18}\text{O} \rightarrow ^{18}\text{O} + ^{16}\text{O}^{16}\text{O}$	k2b = 1.34×10^{-12}
	R(2c)	$^{17}\text{O} + ^{16}\text{O}^{16}\text{O} \rightarrow ^{16}\text{O} + ^{16}\text{O}^{17}\text{O}$	k2c = 2.90×10^{-12}
	R(2d)	$^{16}\text{O} + ^{16}\text{O}^{17}\text{O} \rightarrow ^{17}\text{O} + ^{16}\text{O}^{16}\text{O}$	k2d = 1.39×10^{-12}
Ozone formation	R(3a)	$^{16}\text{O} + ^{16}\text{O}^{16}\text{O} + \text{M} \rightarrow ^{16}\text{O}^{16}\text{O}^{16}\text{O} + \text{M}$	k3a = 6.0×10^{-34}
	R(3b)	$^{16}\text{O} + ^{16}\text{O}^{18}\text{O} + \text{M} \rightarrow ^{16}\text{O}^{16}\text{O}^{18}\text{O} + \text{M}$	k3b = $0.5 \times \mathbf{A} \times k3a$
	R(3c)	$^{16}\text{O} + ^{16}\text{O}^{18}\text{O} + \text{M} \rightarrow ^{16}\text{O}^{18}\text{O}^{16}\text{O} + \text{M}$	k3c = $0.5 \times \mathbf{B} \times k3a$
	R(3d)	$^{18}\text{O} + ^{16}\text{O}^{16}\text{O} + \text{M} \rightarrow ^{16}\text{O}^{16}\text{O}^{18}\text{O} + \text{M}$	k3d = $0.92 \times k3a$
	R(3e)	$^{18}\text{O} + ^{16}\text{O}^{16}\text{O} + \text{M} \rightarrow ^{16}\text{O}^{18}\text{O}^{16}\text{O} + \text{M}$	k3e = $0.006 \times k3a$
	R(3f)	$^{16}\text{O} + ^{16}\text{O}^{17}\text{O} + \text{M} \rightarrow ^{16}\text{O}^{16}\text{O}^{17}\text{O} + \text{M}$	k3f = $0.5 \times \mathbf{C} \times k3a$
	R(3g)	$^{16}\text{O} + ^{16}\text{O}^{17}\text{O} + \text{M} \rightarrow ^{16}\text{O}^{17}\text{O}^{16}\text{O} + \text{M}$	k3g = $0.5 \times \mathbf{D} \times k3a$
	R(3h)	$^{17}\text{O} + ^{16}\text{O}^{16}\text{O} + \text{M} \rightarrow ^{16}\text{O}^{16}\text{O}^{17}\text{O} + \text{M}$	k3h = $1.00 \times k3a$
	R(3i)	$^{17}\text{O} + ^{16}\text{O}^{16}\text{O} + \text{M} \rightarrow ^{16}\text{O}^{17}\text{O}^{16}\text{O} + \text{M}$	k3i = $0.006 \times k3a$
Ozone dissociation	R(4a)	$^{16}\text{O}^{16}\text{O}^{16}\text{O} \rightarrow ^{16}\text{O} + ^{16}\text{O}^{16}\text{O}$	k4a = 1.00×10^{-5}
	R(4b)	$^{16}\text{O}^{16}\text{O}^{18}\text{O} \rightarrow ^{18}\text{O} + ^{16}\text{O}^{16}\text{O}$	k4b = $0.5 \times 0.972 \times k4a$
	R(4c)	$^{16}\text{O}^{16}\text{O}^{18}\text{O} \rightarrow ^{16}\text{O} + ^{16}\text{O}^{18}\text{O}$	k4c = $0.5 \times k4a$
	R(4d)	$^{16}\text{O}^{18}\text{O}^{16}\text{O} \rightarrow ^{16}\text{O} + ^{16}\text{O}^{18}\text{O}$	k4d = $0.972 \times k4a$
	R(4e)	$^{16}\text{O}^{16}\text{O}^{17}\text{O} \rightarrow ^{17}\text{O} + ^{16}\text{O}^{16}\text{O}$	k4e = $0.5 \times 0.988 \times k4a$
	R(4f)	$^{16}\text{O}^{16}\text{O}^{17}\text{O} \rightarrow ^{16}\text{O} + ^{16}\text{O}^{17}\text{O}$	k4f = $0.5 \times k4a$
	R(4g)	$^{16}\text{O}^{17}\text{O}^{16}\text{O} \rightarrow ^{16}\text{O} + ^{16}\text{O}^{17}\text{O}$	k4g = $0.988 \times k4a$

consistency in the isotope ratios in atomic species and molecular species but the mismatch is smaller than fraction of 1‰ and is neglected. The mismatch is even less for the isotope anomaly.

B. Choice of rate constants of the reactions

The Kintecus program requires as input the rates of the above 23 reactions along with the concentration of the reactants (namely $^{16}\text{O}^{16}\text{O}$, $^{16}\text{O}^{17}\text{O}$ and $^{16}\text{O}^{18}\text{O}$). The rates of discharge and ozone dissociation were estimated by comparing the yield of ozone in the experiments with the value predicted by the model. We chose the overall rates of dissociation and formation of O_2 and O_3 in such a way that for a 30 min discharge period we obtain typically 80 μmole of ozone when the initial amount of O_2 is $5.5 \times 10^4 \mu\text{mole}$ (100 Torr in a 10 L chamber kept at 293 K). The 80 μmole of ozone corresponds to about 0.14% of the initial oxygen and is typically the amount obtained in most of the experiments discussed above.

C. Fractionation in ozone dissociation

During ozone dissociation, the rates of formation of ^{16}O , ^{17}O , and ^{18}O atoms are not the same due to difference in bond energies of $^{16}\text{O}-^{18}\text{O}$ and $^{16}\text{O}-^{17}\text{O}$ bonds. We used factors of 0.972 and 0.988 for $^{16}\text{O}-^{18}\text{O}$ and $^{16}\text{O}-^{17}\text{O}$ bond dissociation relative to $^{16}\text{O}-^{16}\text{O}$ bond following Wen and Thiemens³⁹ and Pandey and Bhattacharya.³³ We also use a factor of 0.5 for rate constants when there are two product reaction channels. We assume that in ozone dissociation the central atom cannot be removed due to high barrier.³⁵

D. Exchange reactions

For the isotope exchange reaction between ^{18}O and $^{16}\text{O}^{16}\text{O}$ the forward rate was taken from Anderson *et al.*² while the backward rate was obtained by dividing the forward rate by equilibrium constant following Kaye and Strobel.²⁰ Exchange rates between ^{17}O and $^{16}\text{O}^{16}\text{O}$ were obtained in a similar way (see Pandey and Bhattacharya³³ for details).

E. Ozone formation reactions

The rates of the nine ozone formation reactions (Table V) comprise the crucial part in the calculations and are not available for all P and T ranges corresponding to the range of $\delta^{18}\text{O}$ values considered here. However, several earlier experimental data corresponding to various channels of ozone formation by Janssen *et al.*¹⁵ can be used as a guide. They obtained rate constant ratios for the four ^{18}O -containing ozone channels (relative to the major channel $^{16}\text{O} + ^{16}\text{O}^{16}\text{O} \rightarrow ^{16}\text{O}^{16}\text{O}^{16}\text{O}$) and showed (see Table V) that these values correspond to an enrichment of $\delta^{18}\text{O} = 128.5\text{‰}$ (corresponding to a pressure of 267 mbar). Bhattacharya *et al.*⁷ used this information to derive the rate constant ratios for the four ^{17}O -containing ozone channels (see Appendix B of their paper). In the present study,

we consider these values as the starting point for choosing the rate constant ratios at other P and T regimes.

The rate constant for the major isotope channel ($^{16}\text{O} + ^{16}\text{O}^{16}\text{O} \rightarrow ^{16}\text{O}^{16}\text{O}^{16}\text{O}$) is taken as $6.00 \times 10^{-34} \text{ cm}^6 \text{ s}^{-1}$ Anderson *et al.*³ and rates of other channels are expressed as factors of this rate (called rate constant ratios). We assume that the major part of the variation in ozone isotopic ratios arises due to variation in the rates in two channels of $^{16}\text{O} + ^{16}\text{O}^{18}\text{O}$ and two channels of $^{16}\text{O} + ^{16}\text{O}^{17}\text{O}$ while the rates in channels of $^{18}\text{O} + ^{16}\text{O}^{16}\text{O}$ and $^{17}\text{O} + ^{16}\text{O}^{16}\text{O}$ remain constant. This assumption is validated using information from two earlier studies. According to Janssen *et al.*¹⁵ the $^{18}\text{O} + ^{16}\text{O}^{16}\text{O}$ can produce $^{18}\text{O}^{16}\text{O}^{16}\text{O}$ with ratio of 0.92 and a negligible ratio of 0.006 leading to $^{16}\text{O}^{18}\text{O}^{16}\text{O}$. Further, it was shown by Guenther *et al.*¹¹ that for ozone formation above 100 mbar, in contrast to the reduction in ratio in the $^{16}\text{O} + ^{18}\text{O}^{18}\text{O}$ reaction (from a large value of 1.50) the smaller ratio 0.92 in $^{18}\text{O} + ^{16}\text{O}^{16}\text{O}$ reaction does not change. We assume the same to be true for both $^{18}\text{O} + ^{16}\text{O}^{16}\text{O}$ and $^{17}\text{O} + ^{16}\text{O}^{16}\text{O}$ channels. Therefore, we have to determine only the rates of “light atom-heavy O_2 ” reactions (total of four reactions) for a range of ozone δ -values (corresponding to different P and T) for use in the model and these are discussed below.

F. Choice of rate constants for four “light atom-heavy O_2 ” reactions

The rate constant ratios for these four reactions must be chosen such that they reproduce the observed isotope ratios in the model predictions for various P and T conditions. In particular, our aim is to derive the above four rate constant ratios for simulating different δ -values corresponding to two hypotheses: (1) When the HGM model is applicable and we have $\Delta^{17}\text{O}(\text{as}) = 1.5 \times \Delta^{17}\text{O}(\text{bulk})$ and (2) When results from the present work are applicable (showing deviation from the HGM model) and we have $\Delta^{17}\text{O}(\text{as}) = 1.142 \times \Delta^{17}\text{O}(\text{bulk}) + 10.426$ (Figure 4). The rate constant ratios were obtained by fitting a range of $\delta^{18}\text{O}$ and $\delta^{17}\text{O}$ values (bulk, symmetric and asymmetric) which obey these two lines. We note that for the same bulk δ -value one can have different $\delta(\text{as})$ and $\delta(\text{s})$ corresponding to the above two cases. The bulk δ -values for which the fit is to be made are first chosen as explained below.

It was mentioned before that in all our experiments we measured the $\delta^{18}\text{O}$, $\delta^{17}\text{O}$, and $\Delta^{17}\text{O}$ values of the initial ozone. A range of such values were obtained by changing both T and P. Unfortunately, the T could not be precisely monitored in our experiments. Therefore, as a starting point of δ -selection we took the enrichment versus pressure variation data summarized by Mauersberger *et al.*²⁵ for pressures ranging from 10 mbar to 12 000 mbar. Our assumption is that irrespective of the way ozone is made the internal distribution would be the same for the same enrichment. We first fitted two smooth curves (one each for ^{17}O and ^{18}O) through the data points and then chose numerical δ -values from these two curves. Nine corresponding pairs of bulk $\delta^{17}\text{O}$, $\delta^{18}\text{O}$ values (ranging in $\delta^{18}\text{O}$ from 24‰ to 128‰ over a pressure range from 12 000 to 50 mbar, respectively) were chosen (Table VI) and corresponding $\Delta^{17}\text{O}(\text{bulk})$ values were obtained by using the equation: $\Delta^{17}\text{O}(\text{bulk}) = \delta^{17}\text{O}(\text{bulk}) - 0.52 \times \delta^{18}\text{O}(\text{bulk})$.

TABLE VI. The isotopic composition of ozone as a function of pressure adapted from a fit to experimental data given by Mauersberger *et al.*²⁵ Also shown are $\delta^{18}\text{O}$ (bulk), the $\Delta^{17}\text{O}$ (bulk), and $\Delta^{17}\text{O}$ (asymm) values obtained using Kintecus model to fit the prediction of HGM model and Present work. The rate constant ratios of the four important reactions (relative to the rate of $^{16}\text{O}^{16}\text{O}^{16}\text{O}$) in forming four heavy ozone species (shown in last four columns) are also shown as A, B, C, and D, respectively. All δ -values are relative to the starting oxygen gas composition used for forming ozone and are given in ‰. Column “diff” indicates difference between A-values of HGM model and present work and so on for B, C, and D values. Typical error for each value is 0.015 (see text). $\Delta^{17}\text{O}$ (bulk) = $\delta^{17}\text{O}$ (bulk) - 0.52* $\delta^{18}\text{O}$ (bulk). $\Delta^{17}\text{O}$ (as) = 1.5* $\Delta^{17}\text{O}$ (bulk) according to the HGM model case. $\Delta^{17}\text{O}$ (as) = 1.142* $\Delta^{17}\text{O}$ (bulk) + 10.426 according to the Present work case. A, B, C, and D refer to the rate constant ratios of ozone formation channels (symm.¹⁸O, asymm.¹⁸O, symm.¹⁷O, asymm.¹⁷O, respectively) relative to $^{16}\text{O} + ^{16}\text{O}^{16}\text{O} \rightarrow ^{16}\text{O}^{16}\text{O}^{16}\text{O}$ channel.

Pressure (mbar)	Experimental data on ozone enrichment			Case to fit □	Asymm $\Delta^{17}\text{O}$	Calculated from Kintecus model			A		B		C		D	
	$\delta^{18}\text{O}$	$\delta^{17}\text{O}$	$\Delta^{17}\text{O}$			Bulk	Bulk	Asymm								
	(‰)	(‰)	(‰)			$\delta^{18}\text{O}$	$\Delta^{17}\text{O}$	$\Delta^{17}\text{O}$	$^{16}\text{O}^{16}\text{O}^{18}\text{O}$	diff	$^{16}\text{O}^{18}\text{O}^{16}\text{O}$	diff	$^{16}\text{O}^{16}\text{O}^{17}\text{O}$	diff	$^{16}\text{O}^{17}\text{O}^{16}\text{O}$	diff
50	128	112.5	45.9	HGM model	68.9	127.9	45.9	68.9	1.460	0.030	1.078	-0.031	1.344	0.028	1.039	-0.029
				Present work	62.8	128.1	46.1	62.8	1.430		1.109		1.316		1.068	
100	115	104.3	44.5	HGM model	66.8	114.7	44.5	66.8	1.428	0.019	1.07	-0.019	1.323	0.021	1.035	-0.021
				Present work	61.2	114.7	44.5	61.2	1.409		1.089		1.302		1.056	
200	100.7	93.1	40.7	HGM model	61.1	100.5	40.7	60.9	1.395	0.027	1.06	-0.027	1.294	0.022	1.03	-0.022
				Present work	56.9	100.5	40.7	56.9	1.368		1.087		1.272		1.052	
400	94	86.1	37.2	HGM model	55.8	93.9	37.2	55.9	1.378	0.029	1.057	-0.030	1.275	0.021	1.028	-0.022
				Present work	52.9	94.3	37.4	53	1.349		1.087		1.254		1.05	
700	88.5	79.2	33.2	HGM model	49.8	88.3	33.2	49.8	1.363	0.031	1.055	-0.031	1.255	0.019	1.027	-0.019
				Present work	48.3	88.3	33.2	48.4	1.332		1.086		1.236		1.046	
1300	83	74.2	31	HGM Model	46.5	83	31	46.5	1.347	0.032	1.055	-0.031	1.24	0.018	1.027	-0.017
				Present work	45.8	82.7	30.8	45.8	1.315		1.086		1.222		1.044	
2400	67.5	61.7	26.6	HGM model	39.9	67.8	26.7	40	1.301	0.020	1.055	-0.019	1.203	0.009	1.027	-0.009
				Present work	40.8	67.5	26.9	40.8	1.281		1.074		1.194		1.036	
5500	38.9	38.8	18.6	HGM model	27.9	39	18.5	27.9	1.225	0.009	1.044	-0.008	1.139	-0.003	1.021	0.003
				Present work	31.7	38.7	18.7	31.8	1.216		1.052		1.142		1.018	
12000	23.7	26.7	14.4	HGM model	21.6	23.5	14.4	21.6	1.184	-0.005	1.038	0.005	1.105	-0.013	1.018	0.013
				Present work	26.9	23.5	14.4	26.9	1.189		1.033		1.118		1.005	

Next, the $\Delta^{17}\text{O}(\text{as})$ and $\Delta^{17}\text{O}(\text{s})$ for these nine pressure values are calculated for the two cases (HGM model and present work) according to the two formulas given above. The target is to simulate these sets of δ -values by choosing proper rate constants.

The Kintecus program was successful to simulate the δ -values in Table VI with reasonable accuracy by suitable choice of the rate constant ratios. The program calculates the number of molecules of species: $^{16}\text{O}^{16}\text{O}^{16}\text{O}$, $^{16}\text{O}^{16}\text{O}^{18}\text{O}$, $^{16}\text{O}^{18}\text{O}^{16}\text{O}$, $^{16}\text{O}^{16}\text{O}^{17}\text{O}$, and $^{16}\text{O}^{17}\text{O}^{16}\text{O}$ at each time step. The values of $\delta^{18}\text{O}(\text{bulk})$, $\delta^{18}\text{O}(\text{as})$, $\delta^{18}\text{O}(\text{s})$, $\delta^{17}\text{O}(\text{bulk})$, $\delta^{17}\text{O}(\text{as})$, and $\delta^{17}\text{O}(\text{s})$ are then calculated from the final numbers at the end of the program. This is done by first calculating the isotopic ratios $^{18}\text{O}/^{16}\text{O}$ and $^{17}\text{O}/^{16}\text{O}$ for bulk, asymmetric, and symmetric species from the corresponding number of molecules. Dividing them by the ratios in the starting oxygen one can obtain the delta (enrichment) values by standard procedure (see Eq. (1); the procedure is also explained in detail in Ref. 28). Starting from the rates mentioned before we varied the rates by trial and error method to fit the values of $\delta^{18}\text{O}$, $\Delta^{17}\text{O}(\text{bulk})$, and $\Delta^{17}\text{O}(\text{as})$ as close to the expected values as possible (usually within 0.1‰). This was done for each of the nine pressure values in Case 1 (HGM model) and for each of the corresponding nine pressure values in Case 2 (Present work) (Table VI). The differences in the rate constants (~ 0.03) between the two cases are not large; they are of the order of 2% and are just marginally greater than the uncertainty in the rate constants (1%) estimated in Sec. VII G. However, since the δ -values are high $\sim 2\%$ difference in the rate constants lead to measurable difference in the δ -values and especially the pattern over the whole range (given by the linear regression) of δ -values change significantly. We believe that the rates given in the rows of “Present Work” in Table VI represent accurately the enrichment in ozone formation over the range 24‰–130‰.

G. Estimation of uncertainty in the rate constant ratios

For ease in discussion symbols A, B, C, and D (Table VI) are used to refer to the rate constant ratios relative to $^{16}\text{O} + ^{16}\text{O}^{16}\text{O} \rightarrow ^{16}\text{O}^{16}\text{O}^{16}\text{O}$ channel where the corresponding reactions are: A: $^{16}\text{O} + ^{16}\text{O}^{18}\text{O} \rightarrow ^{16}\text{O}^{16}\text{O}^{18}\text{O}$; B: $^{16}\text{O} + ^{16}\text{O}^{18}\text{O} \rightarrow ^{16}\text{O}^{18}\text{O}^{16}\text{O}$; C: $^{16}\text{O} + ^{16}\text{O}^{17}\text{O} \rightarrow ^{16}\text{O}^{16}\text{O}^{17}\text{O}$; D: $^{16}\text{O} + ^{16}\text{O}^{17}\text{O} \rightarrow ^{16}\text{O}^{17}\text{O}^{16}\text{O}$. When using the Kintecus model the rate constant ratios of these four ozone formation channels at various pressures are inferred based on trial and error method and are subject to some uncertainty. The initial choice is based on fitting literature data on pressure variation of bulk δ -values during ozone formation. These values are then slightly modified to fit the site specific data obtained in the present experiment (Table VI).

The pressure (for pure oxygen gas) variation data as available in Mauersberger *et al.*²⁵ has large scatter not only due to experimental limitations but also due to the fact that it combines data from various methods and sources. The high pressure region is especially different from the prediction based on hindered rotor (see Figure 8 in Gao and Marcus¹⁰) unlike the low pressure region. As mentioned before, to

obtain a consistent set of pressure variation data in digital form that can be used as input to the Kintecus program we fitted a smooth curve through the points and read out the δ -values at each of the nine pressures (50, 100, 200, 400, 700, 1300, 2400, 5500, and 12 000 mbar). Based on the smoothing error and the dispersion associated with the data points we estimate that each of the ozone δ -values should have an uncertainty of about $\pm 5\%$. Since we are using these δ -values to derive the coefficients A, B, C, and D values they should also have corresponding uncertainties in them. To determine these uncertainties we used the Kintecus program itself and varied the values of A, B, C, and D to match the higher and lower limit of ozone δ -values in each case. A reasonable estimate of the total error in each can then be obtained by using half of the difference between the corresponding higher and lower values of the coefficients. As an example, at 200 Torr pressure the experimental $\delta^{17}\text{O}$ and $\delta^{18}\text{O}$ values (in ‰) are 93.1 and 100.7 with fitted values of 93.0 and 100.5 corresponding to A and C values of 1.395 and 1.294. Assigning uncertainty of 5‰ in both $\delta^{17}\text{O}$ and $\delta^{18}\text{O}$ values we obtain uncertainty of 0.015 in each of the above values, i.e., 1.395 ± 0.015 and 1.294 ± 0.015 (Table VI). For comparison, the difference between the A values corresponding to 50 and 12 000 mbar is: $1.460 - 1.184 = 0.276$. So the uncertainty in the A value in this case is of the order of 10% of the total variation between the low pressure limit and the high pressure limit. The calculations also show that 0.015 uncertainty applies reasonably well for each of the rate constant ratios in Table VI.

VIII. DYNAMICS AS THE ORIGIN OF THE DEVIATION FROM THE 1.5 RULE

The rate constant ratios change in going from the fit for HGM model to the fit for Present work. For example, for forming $^{16}\text{O}^{16}\text{O}^{18}\text{O}$ -type ozone at high enrichment of 128.0‰ in $\delta^{18}\text{O}$, A decreases from 1.460 to 1.430 while for forming $^{16}\text{O}^{18}\text{O}^{16}\text{O}$ -type ozone B increases correspondingly from 1.078 to 1.109 (Table VI). The changes are such that A + B remain constant at 2.538. The same is true for $^{16}\text{O}^{16}\text{O}^{17}\text{O}$ and $^{16}\text{O}^{17}\text{O}^{16}\text{O}$ type ozone and the C + D remain constant at 2.383. It is clear that the isotope enrichment at the asymmetric position decreases and that in the symmetric position increases by exactly a proportional amount which is expected since the bulk enrichment has to remain constant. The same applies for isotope anomaly. The anomaly in asymmetric position decreases and that in the symmetric position increases to compensate for the decrease. The reverse is true when we consider lower enrichment (less than 24‰). These results show how the rate constants (calculated based on the Kintecus model) change when one takes experimental relation between site specific anomalies in to account. The change is small ($\sim 2\%$) but is the first clear demonstration of a departure from a pure statistical model of ozone formation.

The reason why symmetric molecules acquire anomaly contrary to the expectation from HGM model can be explored when we consider ozone formation reaction in association with isotope exchange reaction, symbolically written as: $X + YZ \rightarrow [XYZ]^* \rightarrow XY + Z$. $[XYZ]^*$ denotes the metastable state of the complex formed by edge-wise

collision of X with molecule YZ. Janssen *et al.*¹⁵ showed that the rate of stabilization of $[XYZ]^*$ to form a molecule XYZ depends on the Zero Point Energy (ZPE) difference of oxygen molecules in the entrance and exit channels, i.e., $\Delta ZPE = ZPE(XY) - ZPE(YZ)$. If ΔZPE is positive (the reaction being endothermic) the rate is higher and vice versa. This was interpreted as a consequence of an increase in the life time of the metastable state when ΔZPE is positive. The rate constant ratio of asymmetric molecule formation was found to correlate with ΔZPE (in cm^{-1}) according to a simple linear correlation: $k = 0.013^* \Delta ZPE + 1.2$. However, the fit of the ΔZPE and the rate constant ratios was not perfect and several points were below the above line (see Figure 1 in Ref. 15). For example, $^{16}\text{O} + ^{16}\text{O}^{18}\text{O} \rightarrow ^{16}\text{O}^{16}\text{O}^{18}\text{O}$ ratio 1.45 was below the fitted line by ~ 0.02 (a deviation of about 1.4%). Moreover, for symmetric molecules such as $^{16}\text{O}^{18}\text{O}^{16}\text{O}$ or $^{16}\text{O}^{17}\text{O}^{16}\text{O}$ the rate observed was much lower (by about 10 to 20% for edge-on collision only); according to the formula given above the ratios should be close to 1.20 (as $\Delta ZPE = 0$ for them) but the actual ratios were close to 1.0. This prompted Schinke *et al.*³⁵ to comment: “if the linear relationship between the rate coefficients for the non-symmetric molecules and ΔZPE has a sound physical basis, the reason for the different behaviors of the symmetric and asymmetric molecules has to be identified.”

To develop the connection between ΔZPE and reaction rate, Babikov *et al.*⁴ studied the life time distribution of metastable states of two pairs of species ($^{16}\text{O}^{18}\text{O}^{18}\text{O}$, $^{18}\text{O}^{16}\text{O}^{18}\text{O}$) and ($^{16}\text{O}^{16}\text{O}^{18}\text{O}$, $^{16}\text{O}^{18}\text{O}^{16}\text{O}$) near the ΔZPE region and found that the distributions favored formation of the molecules (both symmetric and asymmetric) through certain channels. For example, $^{16}\text{O} + ^{18}\text{O}^{18}\text{O}$ (channel A) is favored over $^{18}\text{O} + ^{16}\text{O}^{18}\text{O}$ (channel B). In contrast, in the second case $^{16}\text{O} + ^{16}\text{O}^{18}\text{O}$ (channel B) is favored over $^{18}\text{O} + ^{16}\text{O}^{16}\text{O}$ (channel A). We note that in both cases the heavier diatom channel is preferred due to its lower ZPE. However, the ratio of the channel A rate to the channel B rate was found to be higher by a factor of about two compared to the experimental result (in the second case). They speculated that neglecting higher than zero J-states (angular momentum) in the calculation causes this discrepancy. In looking for a physical mechanism, they suggested that a second factor, namely a centrifugal barrier effect, would possibly come in to play with larger rotation (due to high J). Interestingly, this barrier works in an opposite direction to the ΔZPE effect. Since there is no calculation for the ^{17}O species it is not possible to talk about $\Delta^{17}\text{O}$ precisely. But the centrifugal barrier effect could be different for ^{17}O - ^{16}O system and the opposing effect then may mean that symmetric molecules such as $^{16}\text{O}^x\text{O}^{16}\text{O}$ would acquire small mass independent enrichment at the expense of the asymmetric ones. With increase in temperature (or decrease in pressure) the rotations of molecules increase with corresponding increase in J and this effect may increase. This special effect acts in conjunction with the ΔZPE effect. Therefore, in this suggestion we have the possibility of acquiring minor amount of $\Delta^{17}\text{O}$ in the symmetric species at the expense of the much larger $\Delta^{17}\text{O}$ in the asymmetric species.

Qualitatively, the ratio of symmetric $\Delta^{17}\text{O}$ to asymmetric $\Delta^{17}\text{O}$ may provide an insight in to the relative importance

of the centrifugal barrier effect to that of the ΔZPE effect. While this speculation can explain the increase in symmetric $\Delta^{17}\text{O}$ at $\Delta^{17}\text{O}(\text{bulk}) > 30$, this cannot give a clue why the symmetric $\Delta^{17}\text{O}$ can become negative at $\Delta^{17}\text{O}(\text{bulk}) < 30$ with corresponding increase in asymmetric $\Delta^{17}\text{O}$ compared to HGM prediction (Figure 4).

IX. A SPECULATION TO EXPLAIN THE OBSERVED DEPARTURE FROM THE 1.5 RULE

The deviation of $\Delta^{17}\text{O}(\text{as})$ from the 1.5 rule, i.e., $\Delta^{17}\text{O}(\text{as}) = 1.5^* \Delta^{17}\text{O}(\text{bulk})$ and $\Delta^{17}\text{O}(\text{s}) = 0$ (Figure 4) can be explained if there is a process acting in association with the one considered in the HGM model which predicts that the isotopic anomaly resides only in the terminal position. We speculate that this deviation is probably due to conversion of asymmetric complex to symmetric complex due to rotation of the diatom in the loosely bound transition state of ozone, first introduced as a *flip effect* by Morgan and Bates³⁰ to explain the higher than expected rate constant ratio for the channel $^{16}\text{O} + ^{16}\text{O}^{18}\text{O} \rightarrow ^{16}\text{O}^{18}\text{O}^{16}\text{O}$. This was also considered a distinct possibility by Janssen *et al.*¹⁵ who analyzed the rate coefficients of various reaction channels forming symmetric and asymmetric molecules. It was found that the symmetric channel associated with the asymmetric channel for the same reactants has a small but finite rate coefficient advantage. For example, in reaction $^{16}\text{O} + ^{16}\text{O}^{18}\text{O}$ formation of $^{16}\text{O}^{16}\text{O}^{18}\text{O}$ with rate 1.45 is associated with formation of $^{16}\text{O}^{18}\text{O}^{16}\text{O}$ with rate 1.08 both of which are mainly end-on process. Janssen *et al.*, however, think that the symmetric rate is slightly enhanced due to “contribution from dynamics which leaves the ad-atom in its end-on position, but mixes exit channels by allowing rotation of the original diatom in the energetic molecule.” They did not calculate the exact magnitude of this enhancement but estimate the amount to be ~ 0.03 surprisingly similar to the value found using the Kintecus model in the present case (see Sec. VII F and Table VI).

The flip effect allows for conversion of asymmetric species to symmetric species. The reverse process should also be allowed (conversion of symmetric species to asymmetric ones) but that rate would be less. This can happen for both ^{18}O and ^{17}O species. The pattern of deviation discussed above requires that the flip effect should also be a function of pressure and temperature. As is well known, with increase in temperature both the enrichment and anomaly of ozone increase and therefore, a clear picture would emerge if the flip effect is discussed in terms of positional isotopic enrichment (i.e., in terms of $\delta^{17}\text{O}$ and $\delta^{18}\text{O}$) and not anomaly only. However, for this we need to derive positional ozone enrichment (in both ^{17}O and ^{18}O) as a function of the bulk anomaly in ozone. As mentioned before, all our data relating the ozone reaction products involve an unknown amount of fractionation and therefore cannot be used directly to derive the positional enrichment.

We can, however, take recourse to the available spectroscopic data on isotopic enrichment (*albeit* with larger uncertainty) which does not have this limitation. The compilation by Janssen¹⁶ is especially useful for this purpose. Based on the available TDLAS data on ^{18}O type ozone Janssen has

shown that the ^{18}O -enrichment in the base and the apex position of ozone can be expressed in terms of bulk enrichment (in ‰ notation) as

$$\delta^{18}\text{O}(\text{as}) = -17.04 + 1.33*\delta^{18}\text{O}(\text{bulk}) - 3.93*10^{-4}*\delta^{18}\text{O}(\text{bulk})^2, \quad (11)$$

$$\delta^{18}\text{O}(\text{s}) = 3*\delta^{18}\text{O}(\text{bulk}) - 2*\delta^{18}\text{O}(\text{terminal}),$$

$$\delta^{18}\text{O}(\text{s}) = 34.08 + 0.34*\delta^{18}\text{O}(\text{bulk}) + 7.86*10^{-4}*\delta^{18}\text{O}(\text{bulk})^2. \quad (12)$$

However, the spectroscopic data on $\delta^{17}\text{O}(\text{as})$ and $\delta^{17}\text{O}(\text{s})$ are not available to the accuracy needed. But we do have mass spectrometric data relating $\delta^{18}\text{O}(\text{bulk})$ with $\Delta^{17}\text{O}(\text{bulk})$ and these can be used along with data on $\Delta^{17}\text{O}(\text{as})$ and $\Delta^{17}\text{O}(\text{s})$. The procedure adopted is as follows: for a given $\Delta^{17}\text{O}(\text{bulk})$ we obtain $\delta^{18}\text{O}(\text{bulk})$ value using the equation given before (see Figure 2) :

$$\delta^{18}\text{O}(\text{bulk}) = 2.78*\Delta^{17}\text{O}(\text{bulk}) - 8.20. \quad (13)$$

From these values we obtain $\delta^{18}\text{O}(\text{as})$ and $\delta^{18}\text{O}(\text{s})$ by Eqs. (11) and (12). As we already know $\Delta^{17}\text{O}(\text{as})$ and $\Delta^{17}\text{O}(\text{s})$ from our experiments we can determine $\delta^{17}\text{O}(\text{as})$ and $\delta^{17}\text{O}(\text{s})$ since

$$\delta^{17}\text{O}(\text{as}) = \Delta^{17}\text{O}(\text{as}) + 0.52*\delta^{18}\text{O}(\text{as}), \quad (14)$$

$$\delta^{17}\text{O}(\text{s}) = \Delta^{17}\text{O}(\text{s}) + 0.52*\delta^{18}\text{O}(\text{s}). \quad (15)$$

For simplicity we use the best fit line (Eq. (12)) rather than individual values and calculate the four positional enrichments for a set of $\Delta^{17}\text{O}(\text{bulk})$ values shown in Figure 5. The uncertainty of the enrichments is obtained by quadratic addition of the uncertainty of $\delta^{18}\text{O}$ from Eq. (12) and the uncertainty given by Janssen¹⁶ associated with the Eqs. (11) and (12). Typical values range from 8‰ to 10‰ (1 σ).

The enrichment in asymmetric ^{18}O -type ozone denoted by $\delta^{18}\text{O}(\text{as})$ is less compared to the symmetric ^{18}O -type,

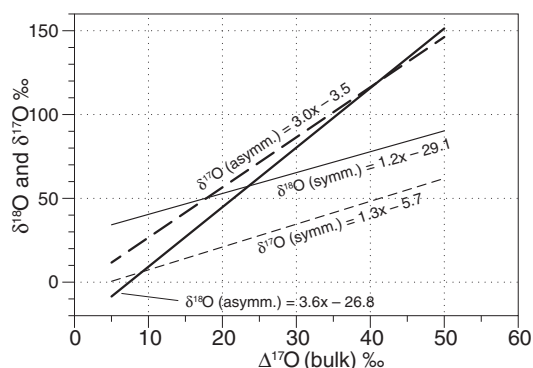


FIG. 5. The variation of $\delta^{18}\text{O}(\text{asymm.})$, $\delta^{18}\text{O}(\text{symm.})$, $\delta^{17}\text{O}(\text{asymm.})$, and $\delta^{17}\text{O}(\text{symm.})$ with bulk ozone isotopic anomaly $\Delta^{17}\text{O}(\text{bulk})$ based on combination of data obtained from the present work and Janssen¹⁶ compilation. The lines are fitted to the calculated points as explained in the text. Note that the “asymmetric” lines are not strictly parallel. And the same is true for the “symmetric” lines. This causes minor changes in $\Delta^{17}\text{O}$ of the asymmetric and symmetric species. At $\Delta^{17}\text{O}(\text{bulk})$ value of about 28‰ the $\delta^{17}\text{O}(\text{symm.})$ is about half of $\delta^{18}\text{O}(\text{symm.})$ and the mass dependence rule of fractionation for symmetric species is obeyed in this special case.

denoted by $\delta^{18}\text{O}(\text{s})$, at $\Delta^{17}\text{O}(\text{bulk})$ values less than 28‰ (Figure 5). For these values the ratio r_{50} (indicative of asymmetric to symmetric ratio for ^{18}O type ozone) as defined earlier is less than the statistical ratio 2.0. The two curves cross each other at about $\Delta^{17}\text{O}(\text{bulk}) \sim 28‰$ after which r_{50} is more than 2.0 (see Table 1 in Ref. 16). The corresponding curves for the ^{17}O -type ozone are also shown in Figure 5 as $\delta^{17}\text{O}(\text{as})$ and $\delta^{17}\text{O}(\text{s})$. In this case also the values increase with $\Delta^{17}\text{O}(\text{bulk})$ but the nature of the increase is significantly different and the two curves cross each other only near zero. The variation of these two indicates that r_{49} (asymmetric to symmetric ratio for ^{17}O type ozone) also increases with $\Delta^{17}\text{O}(\text{bulk})$ values as in case of r_{50} but the pattern of the increase is different. If the difference is due to a flip effect it would indicate that the flip effect of ^{17}O -species is different from that of ^{18}O -species. This feature is a direct consequence of the departure from the 1.5 rule.

The flip effect can be considered as a *leakage* of heavy isotopes from asymmetric species to symmetric one. This leakage should be a function of temperature and must depend on the isotopic species. If asymmetric to symmetric *leakage* is lower for ^{18}O -species compared to the ^{17}O -species the $\Delta^{17}\text{O}(\text{as})$ would decrease. To explain our observation in this context, we require that initially at low temperature (near about 100 K) *leakage* for ^{18}O -species is higher than that of ^{17}O -species and with increase in temperature the relative leakage reverses and becomes lower. As suggested by Morgan and Bates³⁰ the leakage is a function of $\nu(\text{F})/\nu(\text{D})$ the frequency of diatom rotation and that of dissociation and this is expected to decrease with temperature. But the extent of decrease should depend inversely on mass of the heavy atom at the end.

X. CONCLUSION

The Hathorn-Gao-Marcus model of isotopic composition of ozone in gas phase reaction of oxygen atoms and molecules predicts that ozone would not only be enriched in heavy isotopes but also the enrichment would be anomalous in the sense that ^{17}O and ^{18}O species of ozone would have similar enrichment violating the mass dependent fractionation law encountered in many natural processes. There are symmetric (with heavy isotope at the apex position) and asymmetric (with heavy isotope at the base position) heavy ozone of both ^{17}O and ^{18}O type. The HGM model also predicts that the anomalous enrichment (defined as $\Delta^{17}\text{O} = \delta^{17}\text{O} - 0.52*\delta^{18}\text{O}$) is expected to have the following relations: $\Delta^{17}\text{O}(\text{as}) = 1.5*\Delta^{17}\text{O}(\text{bulk})$ and $\Delta^{17}\text{O}(\text{s}) = 0$ for all values of the enrichment. We have summarized data from four experiments which were designed to test this prediction and find that there is small ($\sim 2\%$) but significant deviation from the prediction at low and high levels of enrichment. At low enrichment values [$\Delta^{17}\text{O}(\text{bulk})$ less than 28‰] the $\Delta^{17}\text{O}(\text{as})$ is more than expected while the reverse is true for higher values. Correspondingly, the $\Delta^{17}\text{O}(\text{s})$ is positive for $\Delta^{17}\text{O}(\text{bulk}) > 28‰$ and negative for $\Delta^{17}\text{O}(\text{bulk}) < 28‰$. The observation for $\Delta^{17}\text{O}(\text{bulk}) > 28‰$ can be explained by a mechanism proposed by Babikov *et al.*⁴ by invoking effect of angular momentum states with $J > 0$ which initiates an extra

barrier due to centrifugal effect and works in reverse direction to that of ΔZPE effect. However, this cannot explain the <28% results. The analysis of experimental data presented here shows that in ozone formation dynamics must play a role which modifies the stabilization behavior of ozone isotopic species. This result provides the first experimental confirmation that formation of ozone deviates from a purely statistical model (constrained by restrictions of symmetry) over certain P and T ranges.

ACKNOWLEDGMENTS

S.K.B. thanks Academia Sinica for providing Fellowship for the duration when the paper was completed.

- ¹Alexander, B., Savarino, J., Kreutz, K. J., and Thiemens, M. H., "Impact of preindustrial biomass-burning emissions on the oxidation pathways of tropospheric sulfur and nitrogen," *J. Geophys. Res.* **109**, D08303, doi:10.1029/2003JD004218 (2014).
- ²Anderson, S. M., Klein, F. S., and Kaufman, F., "Kinetics of the isotope exchange reaction of ^{18}O with NO and O_2 at 298 K," *J. Chem. Phys.* **83**, 1648 (1985).
- ³Anderson, S. M., Hulsebusch, D., and Mauersberger, K., "Surprising rate coefficient for four isotopic variants of $\text{O} + \text{O}_2 + \text{M}$," *J. Chem. Phys.* **107**(14), 5385 (1997).
- ⁴Babikov, D., Kendrick, B. K., Walker, R. B., Pack, R. T., Fleurat-Lesard, P., and Schinke, R., "Formation of ozone: metastable states and anomalous isotope effect," *J. Chem. Phys.* **119**(51), 2577–2589 (2003).
- ⁵Berhanu, T. A., Savarino, J., Bhattacharya, S. K., and Vicars, W. C., "O-17 excess transfer during the $\text{NO}_2 + \text{O}_3 \rightarrow \text{NO}_3 + \text{O}_2$ reaction," *J. Chem. Phys.* **136**(4), 044311 (2012).
- ⁶Bhattacharya, S. K., Savarino, J., and Luz, B., "Mass dependent isotopic composition in ozone produced by electrolysis," *Anal. Chem.* **81**, 5226–5232 (2009).
- ⁷Bhattacharya, S. K., Pandey, A., and Savarino, J., "Determination of intramolecular isotope distribution of ozone by oxidation reaction with silver metal," *J. Geophys. Res., [Atmos.]* **113**, D03303, doi:10.1029/2006JD008309 (2008).
- ⁸Gao, Y. Q. and Marcus, R. M., "An approximate theory of the ozone isotope effects: rate constants and pressure dependence," *J. Chem. Phys.* **127**, 244316 (2007).
- ⁹Gao, Y. Q. and Marcus, R. A., "Strange and unconventional isotope effects in ozone formation," *Science* **293**, 259–263 (2001).
- ¹⁰Gao, Y. Q. and Marcus, R. A., "On the theory of the strange and unconventional isotope effects in ozone formation," *J. Chem. Phys.* **116**, 137–154 (2002).
- ¹¹Guenther, J., Erbacher, B., Krankowsky, D., and Mauersberger, K., "Pressure dependence of two relative ozone formation rate coefficients," *Chem. Phys. Lett.* **306**, 209–213 (1999).
- ¹²Hathorn, B. C. and Marcus, R. A., "An intramolecular theory of the mass-independent isotope effect for ozone I," *J. Chem. Phys.* **111**(9), 4087–4100 (1999).
- ¹³Hathorn, B. C. and Marcus, R. A., "An intramolecular theory of the mass-independent isotope effect for ozone. Numerical implementation at low pressures using a loose transition state II," *J. Chem. Phys.* **113**(21), 9497–9509 (2000).
- ¹⁴Ianni, J., KINTECUS, Vast Technologies Development, Inc., Kintecus License Division 26, Willowbrook Ave, Lansdowne, PA 19050, 2013, see www.kintecus.com.
- ¹⁵Janssen, C., Guenther, J., Mauersberger, K., and Krankowsky, D., "Kinetic origin of the ozone isotope effect: a critical analysis of enrichments and rate coefficients," *Phys. Chem. Chem. Phys.* **3**(21), 4718–4721 (2001).
- ¹⁶Janssen, C., "Intramolecular isotope distribution in heavy ozone ($^{16}\text{O}^{18}\text{O}^{16}\text{O}$ and $^{16}\text{O}^{16}\text{O}^{18}\text{O}$)," *J. Geophys. Res.* **110**, D08308, doi:10.1029/2004JD005479 (2005).
- ¹⁷Janssen, C. and Tuzson, B., "A diode laser spectrometer for symmetry selective detection of ozone isotopomers," *Appl. Phys. B* **82**, 487–494 (2006).
- ¹⁸Janssen, C. and Tuzson, B., "Isotope evidence for ozone formation on surfaces," *J. Phys. Chem. A* **114**, 9709–9719 (2010).
- ¹⁹Jacobs, H., Miethke, F., Rutscher, A., and Wagner, H. E., "Reaction kinetics and chemical quasi-equilibria of the ozone synthesis in oxygen DC discharge," *Contrib. Plasma Phys.* **36**(4), 471–486 (1996).
- ²⁰Kaye, J. A. and Strobel, D. F., "Enhancement of heavy ozone in the Earth's atmosphere," *J. Geophys. Res.* **88**(C13), 8447–8452, doi:10.1029/JC088iC13p08447 (1983).
- ²¹Kunasek, S. A., Alexander, B., Steig, E. J., Hastings, M. G., Gleason, D. J., and Jarvis, J. C., "Measurements and modeling of $\Delta^{17}\text{O}$ of nitrate in snowpits from Summit, Greenland," *J. Geophys. Res.* **113**, D24302, doi:10.1029/2008JD010103 (2008).
- ²²Liang, M. C., Irion, F. W., Weibel, J. D., Miller, C. E., Blake, G. A., and Yung, Y. L., "Isotopic composition of stratospheric ozone," *J. Geophys. Res., [Atmos.]* **111**(D2), D02302, doi:10.1029/2005JD006342 (2006).
- ²³Liu, Q., Schurter, L. M., Muller, C. E., Aloisio, S., Francisco, J. S., and Margerum, D. W., "Kinetics and mechanisms of aqueous ozone reactions with bromide, sulfite, hydrogen sulfite, iodide, and nitrite ions," *Inorg. Chem.* **40**, 4436–4442 (2001).
- ²⁴Marcus, R., "Mass-independent oxygen isotope fractionation in selected systems. Mechanistic considerations," *Adv. Quant. Chem.* **55**, 5 (2008).
- ²⁵Mauersberger, K., Krankowsky, D., Janssen, C., and Schinke, R., "Assessment of the ozone isotope effect," *Adv. At., Mol., Opt. Phys.* **50**, 1–54, (2005).
- ²⁶Michalski, G., Scott, Z., Kabling, M., and Thiemens, M., "First measurements and modeling of $\Delta^{17}\text{O}$ in atmospheric nitrate," *Geophys. Res. Lett.* **30**(16), 1870, doi:10.1029/2003GL017015 (2003).
- ²⁷Michalski, G. and Bhattacharya, S. K., "The role of symmetry in the mass independent isotope effect in ozone," *Proc. Natl. Acad. Sci. U.S.A.* **106**(14), 5493 (2009).
- ²⁸Michalski, G., Bhattacharya, S. K., and Girsch, G., "NOx cycle and the tropospheric ozone isotope anomaly: an experimental investigation," *Atmos. Chem. Phys.* **14**, 4935–4953 (2014).
- ²⁹Miller, F. M., "Isotopic fractionation and the quantification of ^{17}O anomalies in the oxygen three-isotope system: an appraisal and geochemical significance," *Geochim. Cosmochim. Acta* **66**(11), 1881–1889 (2002).
- ³⁰Morgan, W. L. and Bates, D., "Stratospheric heavy ozone: the symmetric isomer," *Planet. Space Sci.* **40**, 1573 (1992).
- ³¹Morin, S., Savarino, J., Bekki, S., Gong, S., and Bottenheim, J. W., "Signature of Arctic surface ozone depletion events in the isotope anomaly: $\delta^{17}\text{O}$ of atmospheric nitrate," *Atmos. Chem. Phys.* **7**, 1451–1469 (2007).
- ³²Morton, J., Barnes, J., Schueler, B., and Mauersberger, K., "Laboratory studies of heavy ozone," *J. Geophys. Res.* **95**, 901, doi:10.1029/JD095iD01p00901 (1990).
- ³³Pandey, A. and Bhattacharya, S. K., "Anomalous oxygen isotope enrichment in CO_2 produced from $\text{O} + \text{CO}$: estimates based on experimental results and model predictions," *J. Chem. Phys.* **124**, 234301 (2006).
- ³⁴Savarino, J., Bhattacharya, S. K., Morin, S., Baroni, M., and Doussin, J. F., "The $\text{NO} + \text{O}_3$ reaction: A triple isotope perspective on the reaction dynamics and atmospheric implications for the transfer of the ozone isotope anomaly," *J. Chem. Phys.* **128**(19), 194303 (2008).
- ³⁵Schinke, R., Grebenschikov, S. Y., Ivanov, M. V., and Fleurat-Lessard, P., "Dynamical studies of the ozone isotope effect: a status report," *Ann. Rev. Phys. Chem.* **57**, 625–661 (2006).
- ³⁶Thiemens, M. H. and Heidenreich, J. E. III, "The mass-independent fractionation of oxygen: a novel isotope effect and its possible cosmochemical implications," *Science* **219**(4588), 1073–1075 (1983).
- ³⁷Tuzson, B., "Symmetry specific study of ozone isotopomer formation," Dissertation, University of Heidelberg, Germany, 2005, see <http://www.ub.uni-heidelberg.de/archiv/5523>.
- ³⁸Tuzson, B. and Janssen, C., "Unambiguous identification of ^{17}O containing ozone isotopomers for symmetry selective detection," *Isot. Environ. Health Stud.* **42**, 67–75 (2006).
- ³⁹Wen, J. and Thiemens, M. H., "Experimental and theoretical study of isotope effects on ozone decomposition," *J. Geophys. Res.* **96**, 10911, doi:10.1029/91JD00388 (1991).